

Geochemical and Sm–Nd isotopic characteristics of the Late Archaean–Palaeoproterozoic Dhanjori and Chaibasa metasedimentary rocks, Singhbhum craton, E. India: Implications for provenance, and contemporary basin tectonics

S. De^{a,e}, R. Mazumder^{a,b,*}, T. Ohta^c, E. Hegner^d, K. Yamada^c, T. Bhattacharyya^e, J. Chiarenzelli^f, W. Altermann^g, M. Arima^h

^a Geological Studies Unit, Indian Statistical Institute, 203, B.T. Road, Kolkata 700108, India

^b School of Biological, Earth and Environmental Sciences and Australian Centre for Astrobiology, University of New South Wales, Kensington, Sydney, NSW 2052, Australia

^c Department of Earth Sciences, School of Education & Integrated Sciences and Art, Waseda University, 1-6-1, Nishiwaseda, Shinjuku-ku, Tokyo 169-8050, Japan

^d Department of Earth and Environmental Sciences and GeoBio Center, Theresienstr. 41, 80333 Munich, Germany

^e Department of Geology, University of Calcutta, 35, Ballygunge Circular Road, Kolkata 700019, India

^f Department of Geology, St. Lawrence University, Canton, NY 13617, USA

^g Department of Geology, University of Pretoria, Pretoria 0002, South Africa

^h Graduate School of Environment and Information Sciences, Yokohama National University, 79-7, Tokiwadai, Hodogaya, Yokohama 240-8501, Japan

ABSTRACT

In significant contrast to other cratonic blocks of India, the Singhbhum cratonic successions record continuous depositional record from the Palaeoarchaean to Mesoproterozoic. Although the sedimentary facies characteristics and mode of stratigraphic sequence building of the Dhanjori and Chaibasa Formations are well known, sedimentary geochemistry, provenance and tectonic milieu of deposition of these two formations are hitherto unknown. The current manuscript presents geochemical and Sm–Nd isotopic data from the Dhanjori and Chaibasa Formations for the first time and combine previous sedimentological data with the goal to expand the framework for understanding the depositional and tectonic setting of these two formations. The Sm–Nd isotopic data for the Chaibasa clastics is unambiguous with respect to provenance. Average ε_{Nd} ($t = 2.2 \text{ Ga}$) = -0.8 ± 1.0 and average Nd model age (TDM) = $2.51 \pm 0.08 \text{ Ga}$ with average $^{147}\text{Sm}/^{144}\text{Nd}$ ratios = 0.1114 ± 0.0041 for phyllites and quartzites indicate an extremely homogeneous source signature consistent with a late Archaean “juvenile” crustal provenance, possibly a dominantly upper crustal provenance. The Sm–Nd isotopic data from the older Dhanjori Formation also indicate broadly similar provenance as comparable lithologies in the younger Chaibasa Formation. Our Sm–Nd isotopic data is entirely consistent with the previous sedimentological data and confirms a terrestrial, rift-dominated tectonic setting for the Dhanjori Formation (proximal sources, poorly mixed provenance) and a marginal marine to offshore setting for the more homogeneous Nd isotopic signature of the Chaibasa Formation (distal sources, well mixed provenance).

Keywords:
Provenance
Sediment geochemistry
Palaeoproterozoic
Tectonics
Palaeoclimate
Singhbhum

1. Introduction

The Singhbhum craton, eastern India (Fig. 1) is among one of the few Precambrian terrains in the world that reportedly records sedimentation and volcanism in a changing tectonic scenario ranging from Palaeo-archaean to Mesoproterozoic (Saha, 1994; Mazumder et al., 2000, 2012a,b; Mukhopadhyay, 2001; Mazumder, 2005; Eriksson et al., 2006; Prabhakar and Bhattacharya, 2013;

* Corresponding author at: Department of Applied Geology, School of Engineering and Science, Curtin University Sarawak, CDT 250, 98009 Miri, Sarawak, Malaysia.
Tel.: +60 0164658246; fax: +60 85 443 837.

E-mail address: rajatunsw@gmail.com (R. Mazumder).

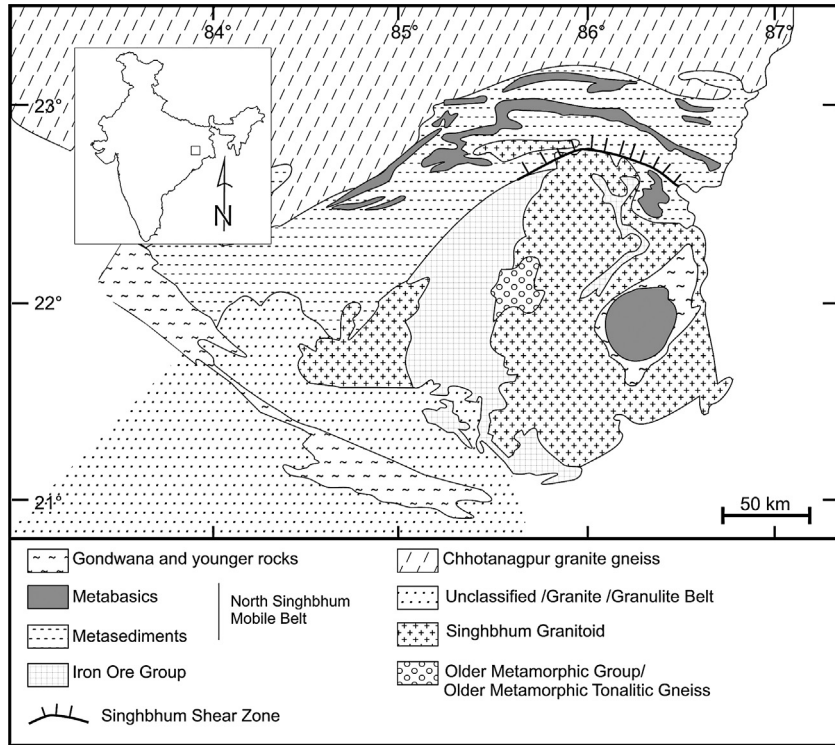


Fig. 1. Geological map of the Singhbhum craton (modified after Mukhopadhyay, 2001). The Singhbhum granitoid and the eastern (E), western (W) and southern (S) Iron Ore Group of rocks constitute the Archaean Singhbhum nucleus (see Mukhopadhyay, 2001 and Mazumder et al., 2012 for details).

Mukhopadhyay et al., 2014; Nelson et al., 2014). The volcano-sedimentary succession occurring to the north of the Archaean Singhbhum nucleus has been inferred to constitute the Singhbhum mobile belt or North Singhbhum Mobile Belt (Saha, 1994; Gupta and Basu, 2000; Sengupta and Chattopadhyay, 2004; Dasgupta, 2004). The Dhanjori Formation represents the lower part of the Late-Archaean to Palaeoproterozoic volcano-sedimentary succession and unconformably overlies the Archaean nucleus. It is entirely siliciclastic and incorporates mostly mafic – and minor felsic volcanics and volcaniclastic rocks (Gupta and Basu, 2000; Mazumder and Sarkar, 2004; Mazumder, 2005). The Dhanjori Formation is conformably overlain by the thicker, and entirely siliciclastic Chaibasa Formation (Mazumder, 2005; Mazumder et al., 2012a,b, 2014).

Determining the depositional and paleotectonic settings of the Dhanjori and Chaibasa Formations is important for understanding the early post-Archaean evolution of the Singhbhum craton. Although earlier researchers studied the sedimentary facies, mode of sedimentary sequence building and stratigraphic relationship between the Dhanjori (Mazumder, 2002; Mazumder and Sarkar, 2004; Mazumder, 2005; Bhattacharya and Mahapatra, 2008; Mazumder and Arima, 2009) and Chaibasa Formation (Bose et al., 1997; Bhattacharya and Bandyopadhyay, 1998; Mazumder, 2002, 2004, 2005; Mallik et al., 2012), issues related to the sediment geochemistry, provenance and tectonic milieu of deposition of these two formations are hitherto unknown (cf. Mazumder et al., 2012a). Chemical and modal composition of the clastic sedimentary rocks provides valuable information for palaeoclimate reconstruction, tectonic setting determination, and provenance analysis (Taylor and McLennan, 1985; Nesbitt and Young, 2004; Saha et al., 2004; Ohta, 2008; Sugitani et al., 2006; Clark et al., 2012). Such information can be extracted by examination of lithology, chemical and isotopic composition of sediments and/or associated volcanic and volcaniclastic rocks (Taylor and McLennan, 1985; McLennan et al., 1993, 2006 and references therein). Efforts have been made to constrain the provenance and tectonic

settings of Archaean and Palaeoproterozoic metasedimentary rocks (McLennan et al., 1983a,b, 1984; Taylor and McLennan, 1995; Fedo et al., 1996, 1997; Saha et al., 2004; Sugitani et al., 2006; Clark et al., 2012). This paper presents geochemical and Sm-Nd isotopic data from the Dhanjori and Chaibasa Formations for the first time to further our knowledge and understanding of the geologic history of the Singhbhum craton with respect to crustal evolution and basin evolution across the Archaean-Palaeoproterozoic transition.

2. Geological setting and geochronology

2.1. Geological setting

The Singhbhum crustal province, encompassing the Singhbhum district Jharkhand and a part of north Orissa, exposes a vast tract of Precambrian rocks occupying an area of approximately 50,000 km² (Figs. 1 and 2). Three distinct petrotectonic zones in the Singhbhum crustal province have been identified. From south to north, these are: (1) the southern Archaean nucleus encompassing various granitoids, Iron Ore Group of rocks, and Late Archaean siliciclastics (cf. Mukhopadhyay, 2001; Mazumder et al., 2012b) (2) the almost 200 km long North Singhbhum Fold Belt comprising the Dhanjori, Chaibasa, Dhalbhum, Dalma and Chandil Formations (cf. Sarkar and Saha, 1962; Gupta and Basu, 1991, 2000; Acharya, 2003), and (3) the extensive granite-gneiss and migmatite terrain in the north, known as the Chhotanagpur Gneissic complex (Figs. 1 and 2).

The Singhbhum Shear Zone (SSZ) occurs close to the northern and eastern margins of the Archaean nucleus and passes very close to the stratigraphic contact between the Dhanjori and Chaibasa Formations (Figs. 1 and 2; see Mukhopadhyay, 1976, 1984; Saha, 1994 and references therein). The Dhanjori Formation has been affected by shearing, and shows an excellent development of strong L-S tectonites in the quartzites, grits and metabasic rocks (Joy and Saha, 1998, 2000). Rocks within the SSZ show the same paragenesis as the Dhanjori Formation except for the presence of kyanite

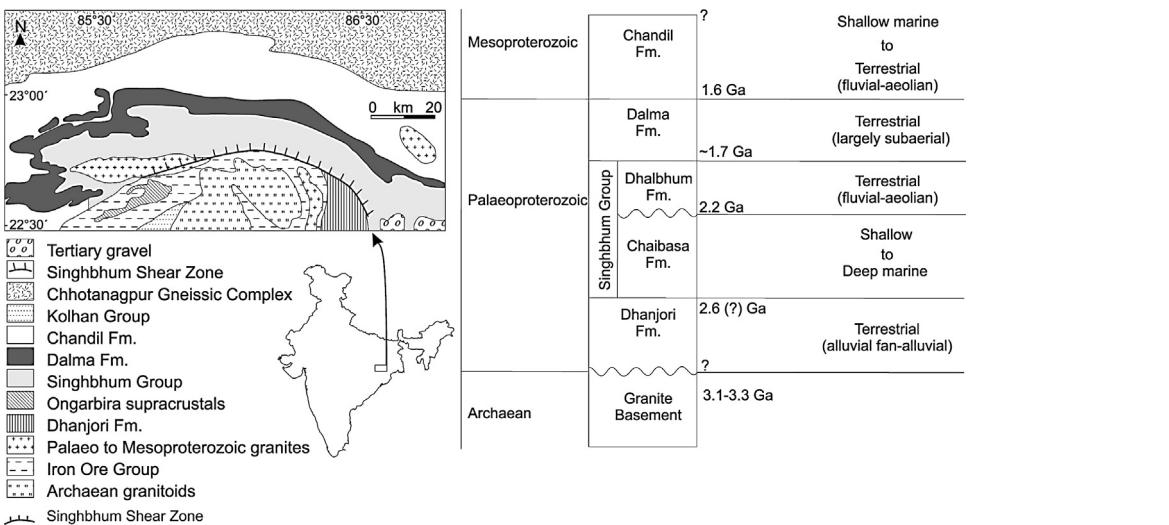


Fig. 2. Simplified geological map showing the disposition of the Dhanjori Formation and the Singhbhum Group (modified after Saha, 1994 and Mazumder, 2005). Geochronological data are presented in the stratigraphic column. See Mazumder et al. (2012a,b) for an updated synthesis of geochronological data.

(Joy and Saha, 2000). The SSZ also affected the Chaibasa Formation (Sengupta and Chattopadhyay, 2004). A difference in opinion exists on various aspects of the SSZ, particularly on its lateral continuity, age of shearing, width and the extent of the rocks that it has affected (cf. Mukhopadhyay, 1984; Saha, 1994; Joy and Saha, 1998, 2000; Sengupta and Chattopadhyay, 2004; Pal et al., 2011; Banerjee and Matin, 2013; Bhattacharya et al., 2014). Mazumder et al. (Mazumder et al., 2012a,b, 2014) presented an updated critical synthesis of the Palaeoproterozoic geological history of the Singhbhum craton and the status of the SSZ that interested reader may find useful.

The Dhanjori Formation is dominantly siliciclastic and incorporates mafic – and minor felsic volcanics and volcaniclastic rocks. The Dhanjori Formation is conformably overlain by the Chaibasa Formation (Sarkar and Deb, 1971; Mukhopadhyay, 1976; Sarkar, 1984; Bose et al., 1997; Mazumder, 2005). The Chaibasa Formation is built of repeated alternations of quartzites (metamorphosed sandstones), heterolithic units (very fine sandstone/shale intercalations) and mica schists (metamorphosed shales) (Bhattacharya, 1991; Bose et al., 1997; Mazumder, 2005). The rocks are metamorphosed to lower greenschist to amphibolite facies (Naha, 1965; Saha, 1994; Ghosh et al., 2006).

2.2. Geochronology

The Sm–Nd isotopic analyses of mafic-ultramafic volcanic rocks from the upper part of the Dhanjori Formation yield an isochron age of 2072 ± 106 Ma indicating their age as Palaeoproterozoic (Roy et al., 2002, p. 510). The age of Dhanjori sedimentation is very poorly constrained and it has been speculated recently that the sedimentation age of the Dhanjori Formation is around 2.6 Ga (see Acharyya et al., 2010a,b and references therein). Based on the age of the Soda Granite underlying the Chaibasa Formation, Sarkar et al. (1986) have inferred that the maximum age of the Chaibasa Formation is ~ 2200 Ma. A SHRIMP U–Pb zircon date of 1861 ± 6 Ma, obtained for the syn- to post-kinematic Arkasani Granophyre that has intruded the SSZ (Bhattacharya et al., 2014). No direct age data is yet available from the metasedimentary rocks of the Palaeoproterozoic supracrustal successions (cf. Mazumder, 2005; Mazumder et al., 2012a) except the Chandil Formation occurring to the north of the Dalma volcanic belt (magmatic zircon SHRIMP concordia age ~ 1600 Ma; Nelson et al., 2007; Reddy et al., 2009; Bhattacharya et al., 2014, Fig. 1). The Dhanjori-Chaibasa succession is thus

tentatively of Late Archaean to Palaeoproterozoic age (Acharyya et al., 2010a,b; Mazumder et al., 2012b, their Table 1).

3. Facies characteristics and depositional setting

As the detailed sedimentary facies analysis of the Dhanjori (Mazumder and Sarkar, 2004; Mazumder, 2005) and Chaibasa (Bhattacharya, 1991; Bose et al., 1997; Mazumder, 2005; Mazumder et al., 2009; Mallik et al., 2012) Formations have been done earlier, we will summarize the salient sedimentary facies characteristics and inferred depositional environments relevant to the sedimentary geochemistry for the sake of brevity. Interested reader may consult Mazumder et al. (2012b) for an overview of Palaeoproterozoic sedimentation in Singhbhum craton.

3.1. Dhanjori Formation

The lower Dhanjori Formation unconformably overlies the Archaean Singhbhum granitoid and is made up of two members: phyllites, quartzites and thin conglomerate comprise the lower member, whereas volcanic and volcaniclastic rocks along with some quartzites and phyllites are important components of the upper member (Fig. 3). The sandstone bodies (Fig. 4a) are either massive or cross-bedded, appear as broadly lenticular, ranging up to 30 m thick. The Dhanjori sandstones are medium to coarse-grained, even locally granule rich and are poorly sorted with matrix content generally 10–12% but at times the matrix content is >15%. Grains, where they retain their primary boundaries, appear subangular to subrounded. Quartz is the most dominant mineral. In addition to quartz, both alkali and plagioclase feldspars are present; plagioclase feldspars often altered to an assemblage of clay and micaceous minerals. The lithic component is represented by quartzite, volcanic rock fragments and rare granitic fragments. The granitic rock fragments are present within the lower part of the Dhanjori succession. In contrast, volcanic rock fragments are confined to the sandstones of the upper part of the Dhanjori succession. In addition, coarser upper Dhanjori sandstones contain siltstone and shale fragments albeit in low frequency (cf. Mazumder and Sarkar, 2004; Mazumder, 2005). Sandstone compositions vary from arkose to feldspathic arenite to lithic arenite/wacke, depending on relative proportion and dominant species of feldspar (cf. Pettijohn, 1975; Bose, 1994; Mazumder and Sarkar, 2004).

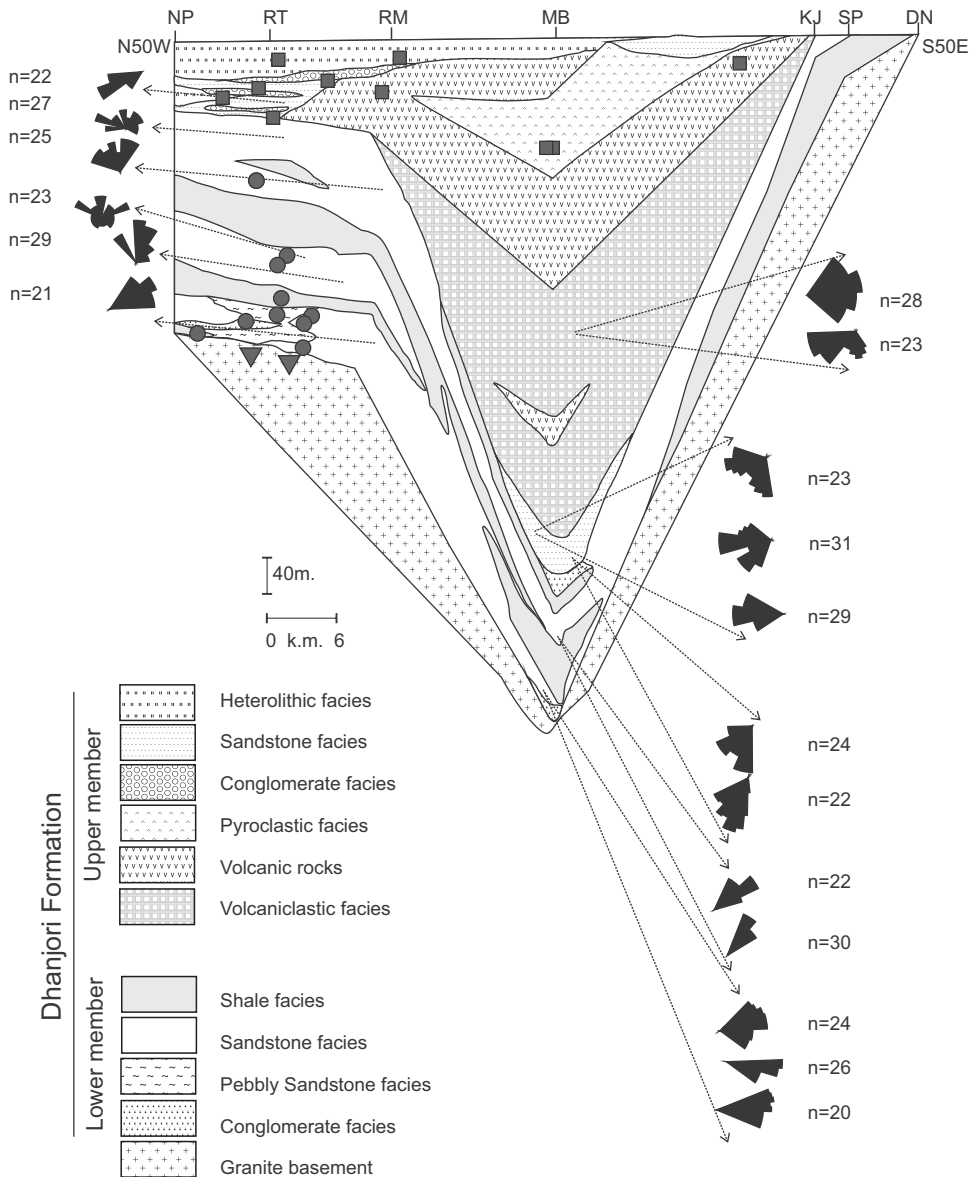


Fig. 3. Panel diagram (modified after Mazumder and Sarkar, 2004) showing lateral and vertical facies transition in Dhanjori Formation with sample locations; inverted triangle = granitoid samples, circle = lower Dhanjori samples, square = upper Dhanjori samples; rectangle = upper Dhanjori volcaniclastic sample. NP = Narwapahar, RT = Rukmini Temple, Jadugorha, RM = Rakha Mines, MB = Moubhander, KJ = Khejurndari, SP = Singpura, DN = Dongadaha; see Mazumder and Sarkar (2004) for details. Note a change in paleocurrent direction between the lower and upper members of the Dhanjori Formation (see Mazumder and Sarkar (2004) for details).

In significant contrast to the Lower Dhanjoris, the upper Dhanjori succession contains thick volcaniclastic facies interbedded with mafic volcanic rocks (Mazumder and Sarkar, 2004, their Fig. 2; Mazumder and Arima, 2009). The clasts are generally sub rounded and their diameter is variable from 0.14 to 25 cm. Vitric tuff containing poorly sorted angular clasts is common.

Poor sediment sorting, compositional immaturity, lenticular geometry and broadly unimodal paleocurrent pattern indicate that the Dhanjori sandstones are fluvial deposits (cf. Miall, 1996; Eriksson et al., 1998; Mazumder and Sarkar, 2004; Mazumder, 2005). The conglomerates formed as mass flow as well as traction current deposits within and without channels (Mazumder and Sarkar, 2004). The conglomerate–sandstone assemblage at the base of the lower member (Figs. 4a and b) has been interpreted as the distal fringe of an alluvial fan deposit (Mazumder and Sarkar, 2004; cf. Blair and McPherson, 1994). The upper member does not include any sheet flood and sieve deposits and is constituted solely by channel and mass flow deposits. This clearly suggests steepening of the

depositional surface. Presence of sedimentary clasts only in the conglomerate assemblages at the base of the Upper Member corroborates steepening of the depositional surface (Mazumder and Sarkar, 2004; Mazumder, 2005).

The upper member of the Dhanjori Formation contains volcanic and volcaniclastic rocks (Fig. 3). Geochemical data of these volcanic and volcaniclastic rocks indicate their generation in an extensional setting and the association of inter-banded terrestrial deposits within the succession constrain its origin in a continental rift setting (Mazumder and Sarkar, 2004; Mazumder and Arima, 2009).

3.2. Chaibasa Formation

Lithologically, the Chaibasa Formation (Fig. 5) is characterized by the interbedding of quartzites (Fig. 6a), a heterolithic (very fine sandstone/siltstone–mudstone; Fig. 6b) and shale facies (Fig. 6c) in different scales. The heterolithic and shale facies is now represented

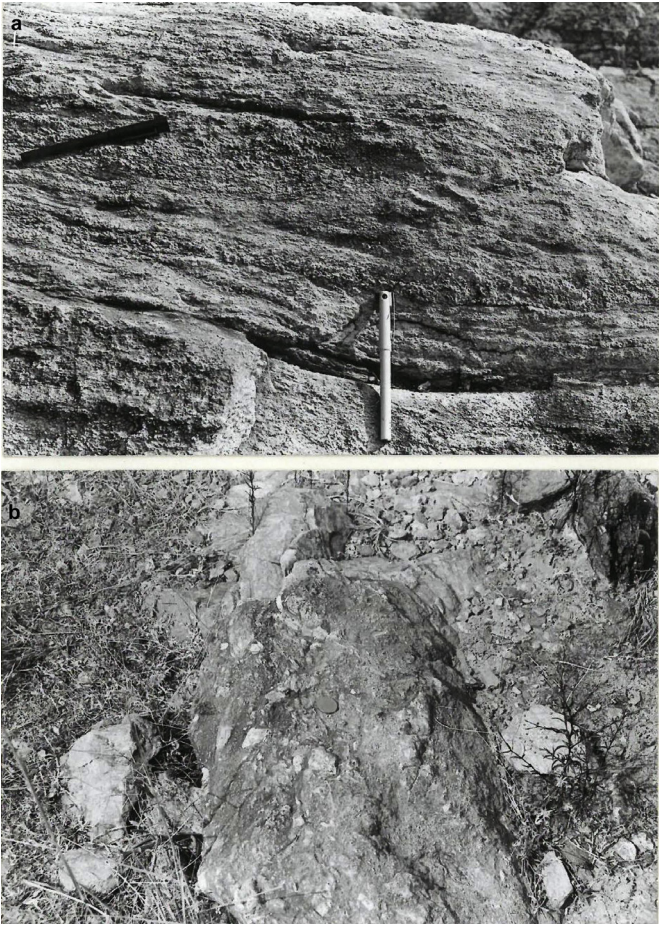


Fig. 4. Field photographs of lower Dhanjori clastics: (a) quartz-pebble bearing quartzose sandstone with stratification and master erosion surface (pen = 12 cm). (b) Conglomerate with highly angular quartz and quartzite pebbles (coin = 1.5 cm).

by schists (Figs. 5 and 6b). It conformably overlies the Dhanjori Formation (cf. Sarkar and Deb, 1971; Mukhopadhyay, 1976; Sarkar, 1984; Mazumder et al., 2012a,b, 2014) and a sheet conglomerate (cf. Mazumder, 2005, his Fig. 8a) or pebbly sandstone (cf. Bose et al., 1997) demarcates the contact (cf. Bose et al., 1997). The sheet conglomerate/pebbly sandstone is exposed in the south-eastern part of the basin where the Chaibasa Formation directly overlies the granitoid basement (see Bose et al., 1997; Mazumder, 2005; Mazumder et al., 2012b, 2014). Bose et al. (1997) have traced the sheet conglomerate/pebbly sandstone along the contact of the Chaibasa and Dhanjori Formations and have noted that the unit becomes thinner towards west. The sheet conglomerate/pebbly sandstone has been interpreted as a transgressive lag deposit and the shale facies of the Chaibasa Formation has been interpreted as a transgressive systems tract (Bose et al., 1997 and references therein; Mazumder, 2005; Mazumder et al., 2012b, 2014).

In significant contrast to the underlying Dhanjori sandstones, the Chaibasa sandstones are very fine- to fine-grained, compositionally as well as texturally mature (Bose et al., 1997; Mazumder, 2005). Quartz is the dominant mineral. In addition, minor muscovite is present as framework mineral. The proportion of matrix is <10%. Compositionally, the Chaibasa sandstones are quartz arenite (cf. Bose et al., 1997; Mazumder, 2005). The sandstone beds are pervasively cross-stratified (Fig. 6a) with spectacular intra set cyclic variation in stratification style (Bose et al., 1997; Mazumder, 2000). Others are partly or completely massive or graded, and a few beds are planar laminated. Locally the sandstone

bed surfaces preserve wave ripples (Mazumder, 1999). Fine grain-size, good sorting, mineralogical as well as textural maturity, local bipolar-bimodal sediment dispersal pattern, and characteristic rhythmicity in the cross-stratification foreset thickness variation (thick-thin alternation) are indicative of the tidal origin of the Chaibasa sandstones (Bose et al., 1997; Mazumder, 2004; Mazumder and Arima, 2005). The heterolithic facies contain profuse wave generated structures including hummocky cross-stratification and numerous slides and slumps implying deposition on a steeper slope in a setting between the fair-weather and storm wave base. The shale facies (Fig. 6c) formed in an offshore setting (Bose et al., 1997; Mazumder et al., 2009; Mallik et al., 2012).

In significant contrast to the lower Chaibasa shale facies formed in a shelf setting below the storm wave base (Bose et al., 1997; Mazumder, 2005) and exposed in the Dhalbhumar-Ghatsila-Moubhandar sector, the upper Chaibasa shale facies exposed in and around Galudih and further north of Galudih bear superimposed ripples and desiccation crack (Bhattacharya, 1991, his Figs. 6 and 12). This implies that the Upper Chaibasa shale facies is of intertidal origin (Bhattacharya, 1991; Bhattacharya and Bandyopadhyay, 1998; Mazumder, 2005). The Chaibasa Formation is thus characterized by a shallowing upward trend (Mazumder, 2005). This is further supported by the presence of terrestrial sediments within the overlying Dhalbhumar Formation (Mazumder, 2005; Mazumder et al., 2012b).

4. Geochemistry

4.1. Analytical methods

Samples (Tables 1–3; see Figs. 3 and 5 for sample locations) for geochemical analyses were collected from least weathered outcrops. After crushing in a metal jaw crusher, all samples were grounded in an agate ball mill. Major, trace and rare earth element abundances were analyzed by Acme Analytical Laboratories in Vancouver, BC, Canada (Table 2). Major elements were analyzed by ICP-OES following a Lithium metaborate/tetraborate fusion and dilute nitric acid digestion. Trace elements and REE were analyzed by ICP-MS following a Lithium metaborate/tetraborate fusion and nitric acid digestion. Precision estimated from duplicate analyses, were better than 2% for major elements. Those for trace elements and REE were better than 7%. Petrographical investigations were performed on a polarizing microscope.

The Sm-Nd isotope compositions were determined in the isotope laboratory at Universität München (Table 3) according to the procedures outlined in Hegner et al. (2010). The $^{143}\text{Nd}/^{144}\text{Nd}$ ratios were determined with a MAT 261 with Spectromat upgraded electronics and control software using a dynamic 2-line triple-mass ion collection method and monitoring ^{147}Sm . Sm isotopes were determined in static data collection mode. The $^{143}\text{Nd}/^{144}\text{Nd}$ ratios are normalized to $^{146}\text{Nd}/^{144}\text{Nd} = 0.7219$ and Sm isotope ratios to $^{147}\text{Sm}/^{152}\text{Sm} = 0.56081$. Sm and Nd concentrations were determined by isotope dilution using a $^{150}\text{Nd}-^{149}\text{Sm}$ tracer solution. External precision for $^{143}\text{Nd}/^{144}\text{Nd}$ is $\sim 1.1 \times 10^{-5}$ (2SD). Error for $^{147}\text{Sm}/^{144}\text{Nd} \sim 0.15\%$ (2SD). The La Jolla Nd standard solution yielded $^{143}\text{Nd}/^{144}\text{Nd} = 0.511847 \pm 8$ (2SD, $N = 10$). The ε_{Nd} values were calculated with the parameter of Bouvier et al. (2008) with present-day values for the chondritic uniform reservoir (CHUR) of $^{147}\text{Sm}/^{144}\text{Nd} = 0.1960$ and $^{143}\text{Nd}/^{144}\text{Nd} = 0.512630$. Model ages were calculated according to DePaolo (1981).

The Chemical Index of Alteration (CIA), the Chemical Index of Weathering (CIW; Harnois, 1988) and the Index of Compositional Variability (ICV; Cox et al., 1995) values have been calculated and the results are presented in Table 4.

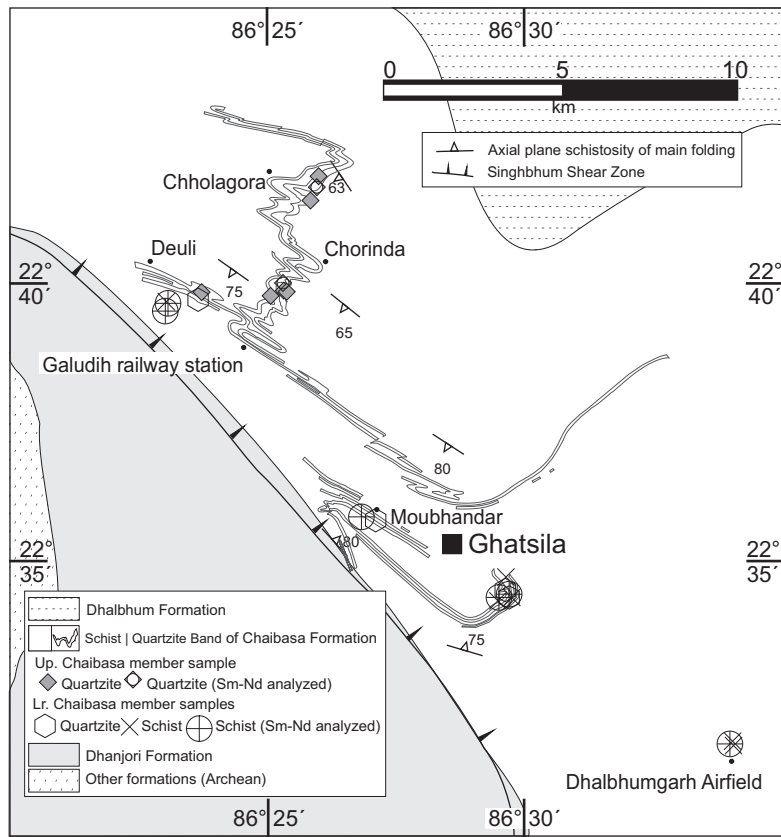


Fig. 5. Geological map (modified after Naha, 1965) showing sampling locations of the Chaibasa clastics. The Singhbhum Shear Zone (SSZ) occurs close to the northern and eastern margins of the Archaean nucleus (Figs. 1 and 2) and passes very close to the contact between the Dhanjori and Chaibasa Formations. The Chaibasa Formation conformably overlies the Dhanjori Formation and the contact between these formations are demarcated by a sheet conglomerate or pebbly sandstone interpreted as a transgressive lag deposit (Bose et al., 1997; Mazumder, 2005; Mazumder et al., 2014). See text for details. The latitude-longitude and relative stratigraphic position of the Chaibasa samples are also shown in Table 1.

4.2. Major, trace and REE characteristics

One approach to determine the protolith of a metamorphosed sedimentary rock is to investigate the major element geochemical characteristics. Herron (1988) proposed the use of an X-Y chart plotting the log of the $\text{Fe}_2\text{O}_3/\text{K}_2\text{O}$ vs. the log of $\text{SiO}_2/\text{Al}_2\text{O}_3$. When plotted on such a graph samples of quartzites of the lower and upper members of both the Dhanjori Chaibasa Formation plot as arenites, arkoses, or wackes (Fig. 7). The Upper Chaibasa arenites cluster largely within the subarkose field along its boundary with sublitharenite and quartz arenite indicative of a quartz-rich arkosic sandstone. In contrast, arenites of the Lower Chaibasa members plot in the lower portion of the diagram from wacke to quartz arenite, indicating variable composition of sand-sized components. Samples of the Upper Dhanjori Formation, with one exception, plot in the quartz arenite field attesting to their quartz-rich composition. In contrast, arenites from the lower Dhanjori members show a similar range of composition to that displayed by the Lower Chaibasa members. The trends shown by arenites in each of the two the Formations indicate increasing textural maturity up section, with arenites of the upper member of Dhanjori Formation the most mature and quartz-rich.

Phyllites of the lower Dhanjori member, upper Dhanjori member, and lower Chaibasa members plot predominantly in the shale to wacke field, with one sample in the subarkosic field and another in the arkosic field (Fig. 7). The lower Chaibasa member phyllites are the most iron-rich and plot predominantly in a cluster spanning the boundary between the shale and wacke field. Samples of upper Dhanjori member phyllite are the most Al and K rich,

plotting near the lower left-hand corner of the diagram and indicating a high phyllosilicate content. Samples of the lower Dhanjori member phyllite plot mostly along the boundary of the wacke and arkosic field that likely indicating a larger portion of sand or silt-sized detritus than the phyllites from other samples. In general, the results confirm petrographic examination and show a wide range of detrital lithologies from phyllosilicate dominated shale to extremely mature quartz arenites. This is well shown by the contrasting location of Upper Dhanjori quartzites and phyllites in Fig. 7.

The REE pattern (Fig. 8a) obtained from the basement granite sample S34 is typical for Archaean tonalitic rocks lacking plagioclase control on crystallization and showing a fractionated HREE pattern. This sample has a high $\text{Na}_2\text{O}/\text{K}_2\text{O}$ ratio of 2.5 supporting a mantle-derived protolith. Basement sample R20 shows a strong positive Eu-anomaly and must be interpreted as a feldspar cumulate.

The REE patterns of the clastics and volcanics (Figs. 8b-f) are generally quite flat, except perhaps some of the upper Dhanjori member rocks, suggesting that the source materials were not too strongly differentiated (Taylor and McLennan, 1985; Rollinson, 1993, 2007). The lower Dhanjori member samples are characterized by restricted range in REE concentrations (Fig. 8b). They show substantial ($\sim 5-50 \times$) enrichment of all the REEs vs. Chondritic values. They also show a LREE enrichment (slight slope from left to right; Fig. 10b), as would be expected from rocks derived by partial melting of mantle (Taylor and McLennan, 1985; Rollinson, 2007). There is little or no indication of Eu anomaly. In comparison to the lower Dhanjori member samples, the upper Dhanjori member

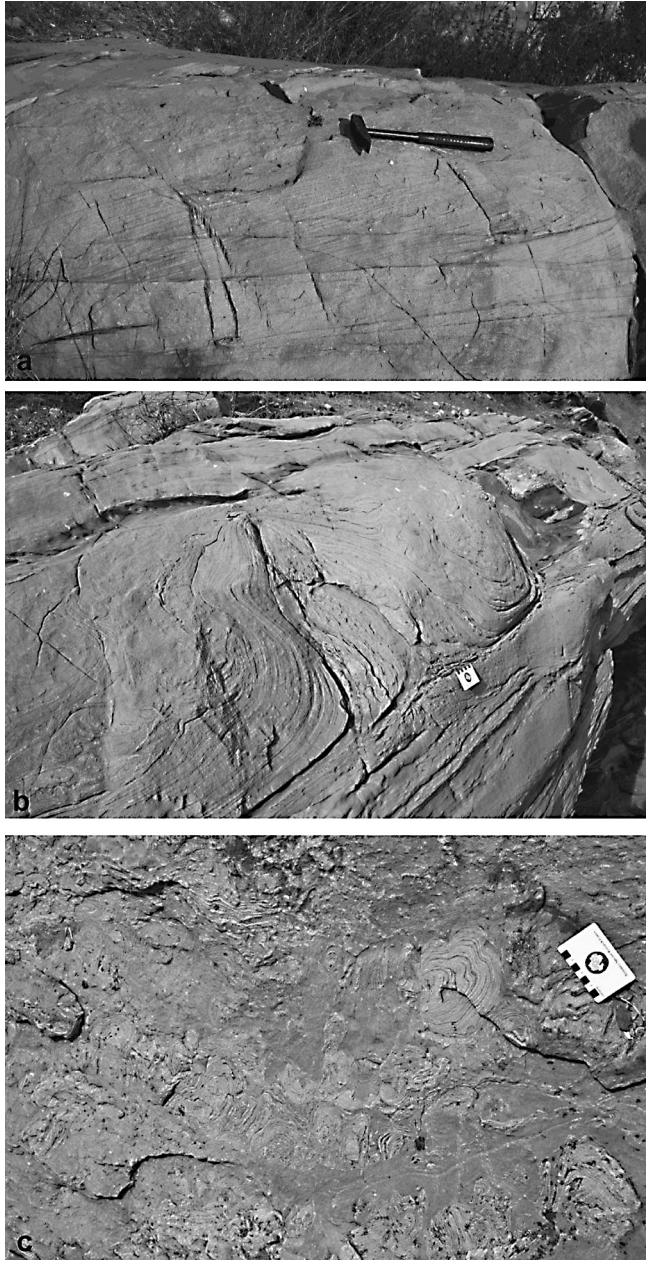


Fig. 6. Field photographs of Chaibasa clastics: (a) cross-bedded Chaibasa sandstone; (b) large convolutes within the sandy units of the heterolithic (sandstone–mudstone) facies; (c) penecontemporaneously deformed chaotic unit within the Chaibasa shale facies. The penecontemporaneously deformed units are laterally persistent and are bounded by undeformed beds and are interpreted as seismites (see [Bose et al., 1997](#); [Bhattacharya and Bandyopadhyay, 1998](#); [Mazumder et al., 2009](#) for details).

samples show a much greater range in REE abundances and patterns ([Figs. 8c and d](#)). This implies variable magmatic sources and dilution by sediments ([Taylor and McLennan, 1985](#)). Several samples appear to have a slight negative Eu anomaly developed, a characteristic of more evolved igneous rocks ([Rollinson, 1993](#); [McLennan et al., 1993](#)). For the bulk of the samples, the pattern is similar to PAAS and other shale composites when normalized to chondritic values suggesting they are a fair representation of Post Archaean Continental Crust ([Taylor and McLennan, 1985](#)).

The Chaibasa REE patterns are flat with no apparent enrichment in light or heavy REEs ([Fig. 8g–i](#)). There is little indication of any anomaly except for Cerium (Ce) ([Fig. 8i](#)). Ce anomalies are supposed

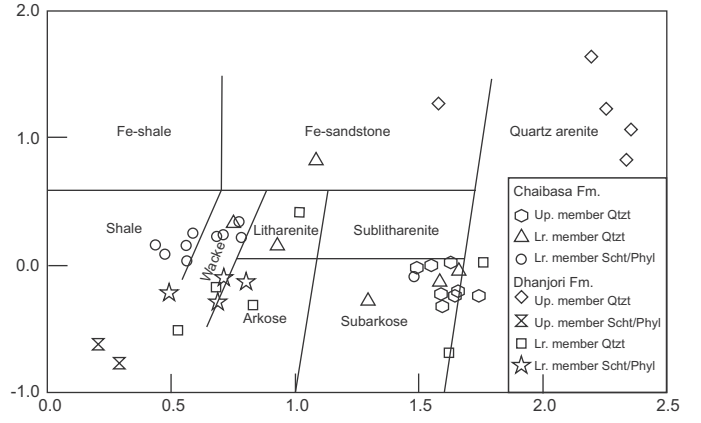


Fig. 7. Log of the $\text{Fe}_2\text{O}_3/\text{K}_2\text{O}$ vs. the log of $\text{SiO}_2/\text{Al}_2\text{O}_3$ plot of Dhanjori and Chaibasa clastics (after [Herron, 1988](#)) to determine the protolith of metamorphosed sedimentary rock. See text for details.

to reflect redox reactions and have been used by some authors to make inferences about atmospheric and terrestrial conditions ([Elderfield and Greaves, 1982](#); and references therein) or sea level change (cf. [Wilde et al., 1996](#)). In the present context, the minor Ce anomaly in lower Chaibasa member finer clastics probably reflects sea level change associated with marine transgression across the Dhanjori-Chaibasa transition ([Bose et al., 1997](#); [Mazumder, 2005](#)).

In the tectonic discrimination diagram of [Roser and Korsch \(1986\)](#), most of the lower Dhanjori member sediments are plotted in the domain of the passive continental margin ([Fig. 9a](#)); three samples plot close to the domain of Active Continental margin whereas all samples of the upper Dhanjori member sediments are within the domain of Passive continental margin ([Fig. 9a](#)). In significant contrast, most of the lower Chaibasa member samples plot in the domain of the Active continental margin and the upper Chaibasa member samples plot within the domain of Passive continental margin ([Fig. 9b](#)). In the tectonic discrimination diagram of [Roser and Korsch \(1988\)](#), both the Dhanjori and Chaibasa samples record upward transition from felsic provenance to mature provenance ([Fig. 9c and d](#)).

In the provenance discrimination diagram of [Ohta \(2008\)](#), both the Dhanjori and Chaibasa samples indicate temporal evolution from intermediate igneous to mature sedimentary provenance ([Fig. 9e and f](#)). While the lower Dhanjori member sediments were derived from a felsic igneous provenance, the lower Chaibasa member sediments were derived from intermediate igneous provenance.

Mixing between felsic and mafic sources can be verified in the $\varepsilon_{\text{Nd}}(t)$ vs. Th/Sc diagram ([Fig. 10](#)), which considers both geochemical and isotopic features of the potential sources. In the $\varepsilon_{\text{Nd}}(t)$ vs. Th/Sc plot, both the Dhanjori and Chaibasa samples plot between arc andesite and upper crust ([Fig. 10a and b](#)). [McLennan et al. \(1993\)](#) noted that sedimentary rocks from modern continental arc and back arc are plotted approximately between arc andesite and upper crust. Unlike the Dhanjori samples, the younger Chaibasa samples are, however, more homogeneous ([Fig. 10a and b](#)). This indicates distant, well mixed provenance for the Chaibasa in contrast to proximal, relatively poorly mixed provenance for the Dhanjoris. In La Th Sc triangular plot ([Fig. 11](#)), the Chaibasa samples show clustering along a median zone between Th-Sc but the Dhanjoris dominantly have a shifting towards high Th values which suggest the contribution from mafic source for the Dhanjoris.

The meta-sedimentary rock samples of the lower and upper member of the Chaibasa Formation have average CIW values of 79.29 and 92.21 ([Table 4](#)) respectively. The lower and upper member clastics of the Dhanjori Formation have average CIW values

Table 1

Relative stratigraphy of the Chaibasa meta-sedimentary rock samples (see Fig.5 for sample locations).

Locality	Latitude	Longitude	Sample No (Lithology)
Chholagora-Bhurisal-Kamarigora	22°41'55" N	86°26'03" E	S 12 (Quartzite)
	22°41'43" N	86°25'59" E	S 13 (Quartzite)
	22°41'29" N	86°25'47" E	S 14 (Quartzite)*
Chorinda-Barbil	22°40'07" N	86°25'28" E	S 15 (Quartzite)
	22°40'00" N	86°25'22" E	S 16 (Quartzite)
	22°39'49" N	86°25'06" E	S 17 (Quartzite)*
	22°39'56" N	86°25'23" E	S 18 (Quartzite)
Deuli-Karanshai-Twin Peak	22°39'55" N	86°23'52" E	S 19 (Quartzite)
Deuli-Karanshai	22°39'42" N	86°23'41" E	S 20 (Quartzite)
Deuli-W. of Chandrarekha (Subarnarekha R. bank)	22°39'32" N	86°23'03" E	S 21 (Heterolithic Schist)*
	22°39'42" N	86°23'06" E	S 22 (Schist)*
	22°39'40" N	86°23'03" E	S 23 (Schist)
Moubhandar	22°35'45" N	86°26'49" E	S 25 (Phyllitic Schist) *
	22°35'40" N	86°27'02" E	S 24 (Quartzite)
Ghatsila- Harindungri	22°34'17" N	86°29'30" E	S 30 (Schist)*
	22°34'14" N	86°29'26" E	S 29 (Heterolithic unit)
	22°34'21" N	86°29'40" E	S 28 (Heterolithic unit)
	22°34'23" N	86°29'39" E	S 27 (Heterolithic unit)*
	22°34'25" N	86°29'31" E	S 32 (Quartzite)
	22°34'18" N	86°29'42" E	S 33 (Quartzite)
	22°34'43" N	86°29'41" E	S 26 (Schist)
Dhalbumgarh Airfield	22°31'41" N	86°34'03" E	S 31 (Heterolithic unit)
	22°31'42" N	86°33'59" E	S 11 (Schist)*
	22°31'42" N	86°34'02" E	S 10 (Schist)

*= Sm-Nd Isotopic analysis

*Sm-Nd isotopic analysis.

of 91.46 and 85.15 (Table 4) respectively. This indicates a strong chemical weathering conditions with terrestrial and marine environment in conformity with worldwide humid warm climate in the Palaeoproterozoic (Eriksson et al., 1998).

Index of compositional variability (ICV; Cox et al., 1995) describes the maturity of the source and the values decrease with increasing degree of weathering. Clastic sedimentary rocks with low ICV values and higher proportion of clay minerals are indicative of recycled and mature sediment provenance in passive margin settings whereas those with high ICV values may indicate an immature source in active tectonic settings (Van de Kamp and Leake, 1985). Quartzite samples of the Lower Chaibasa member show lower ICV values (0.526–0.659; see Table 4) but the samples close to the transition between the lower and upper members of the Chaibasa Formation and the quartzite samples of the upper member of the Chaibasa Formation show much higher values (Table 4). This clearly supports the inference of Mazumder (2005) who proposed a change from passive to active tectonic setting (cf. Van de Kamp and Leake, 1985). The ICV values of sedimentary rocks close to 1 indicate fresh granitoid provenance (Potter et al., 2005). The ICV values of the lower Dhanjori samples (~1) indicates Archaean Singhbhum granitoid provenance.

4.3. Sm-Nd isotopic characteristics

For provenance analysis we preferentially analyzed phyllite (pelitic) material because it represents a large-scale sample of the

exposed crust and reflects its LREE and Nd isotopic characteristics (e.g., Taylor and McLennan, 1985). A few quartzite samples, recording a locally important input, were included from sections where pelitic material was absent. Due to the possibility of accessory minerals in quartzite, they may have erratic REE patterns not representative of the large-scale composition of the source (e.g., Taylor and McLennan, 1985). In addition we have analyzed a tonalitic gneiss sample from the ca. 3.3 Ga old basement (Singhbhum granitoid phase III, see Saha, 1994; Reddy et al., 2009; Mazumder et al., 2012a) (Table 3).

For the metasedimentary samples Nd model ages were calculated after DePaolo (1988a,b) and these data are interpreted as average crustal residence times of the material. For calculation of initial ε_{Nd} values we assumed an average depositional age of 2.2 Ga for the Chaibasa Formation and 2.5 Ga for the underlying Dhanjori Formation. The latter age is interpreted as a maximum value for deposition considering the fact that the youngest calculated Nd model ages in two phyllite samples are ca. 2.5 Ga (samples S4, R12; Table 3). In other words, if the DePaolo model is applicable, the 2.5 Ga Nd model can be interpreted as evidence for 100% of the material in these samples as mantle-derived at ca. 2.5 Ga. Typically, sedimentary rocks contain recycled older crustal material, in this case from the ca. 3.3 Ga basement (Singhbhum granitoid phase III or still older Older Metamorphic Tonalitic gneiss, see Saha, 1994, Acharyya et al., 2010a, Mazumder et al., 2012a and Hofmann and Mazumder, 2014 for details) so that their model age represents an average value for the times when material was derived from the

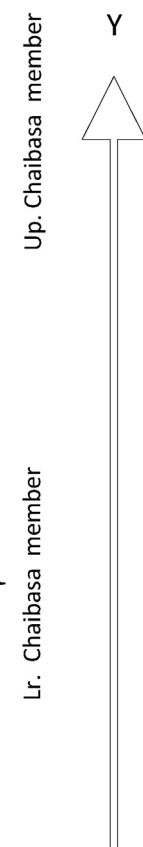


Table 2

Major- and trace element concentrations of Palaeoproterozoic Dhanjori and Chaibasa Formations, Singhbhum craton, eastern India.

Formation	S12	S13	S14	S15	S16	S17	S18	S19	S20	S21	S22	S23	S25	S24	S30	S29	S28	S27	S32	S33	S26	S31	S11	S10
Lithology	Upper Chaibasa												Lower Chaibasa											
	Qtzt.	Qtzt.	Qtzt.	Qtzt.	Qtzt.	Qtzt.	Qtzt.	Qtzt.	Qtzt.	Scht.	Scht.	Scht.	Phyl.	Qtzt.	Scht.	Qtzt.	Ht. Sch.	Ht.Qt.	Qtzt.	Qtzt.	Scht.	Qtzt.	Scht.	Scht.
SiO ₂	94.33	94.37	93.95	93.47	94.65	94.74	94.86	93.52	95.02	73.67	71.50	59.97	57.00	89.32	74.89	73.08	80.62	65.13	94.74	92.98	66.02	84.38	71.12	64.51
TiO ₂	0.05	0.07	0.06	0.06	0.10	0.06	0.05	0.07	0.07	0.48	0.58	0.90	0.96	0.12	0.56	0.50	0.27	0.69	0.07	0.15	0.79	0.19	0.64	0.77
Al ₂ O ₃	2.42	2.16	2.44	2.65	2.25	2.09	1.73	3.02	2.08	12.47	13.96	20.18	20.87	4.54	12.35	12.96	9.50	17.89	2.48	3.09	17.11	6.95	14.83	17.85
Fe ₂ O ₃	0.51	0.57	0.63	0.67	0.64	0.48	0.42	0.65	0.55	4.57	3.81	6.15	7.78	1.01	3.95	4.54	2.37	4.84	0.64	0.90	6.24	2.92	5.30	5.81
MnO	0.01	b.d.	0.07	0.07	0.07	0.17	0.01	0.06	0.05	0.03	0.08	b.d.	b.d.	0.09	0.05	0.05	0.09							
MgO	0.10	0.07	0.13	0.08	0.06	0.12	0.23	0.13	0.12	0.91	0.87	1.24	1.80	0.13	0.94	1.24	0.77	1.06	0.25	0.30	1.27	0.51	1.30	1.46
CaO	0.04	0.10	0.28	b.d.	b.d.	b.d.	0.02	b.d.	b.d.	1.07	1.46	0.64	0.51	0.15	0.83	1.09	0.67	0.85	0.02	0.01	0.65	1.54	0.71	0.91
Na ₂ O	0.09	0.17	0.07	0.01	0.01	0.02	0.07	0.04	0.01	1.87	2.26	1.30	0.97	0.61	1.79	2.37	2.20	2.31	0.08	0.02	1.32	1.90	1.30	1.59
K ₂ O	1.07	1.00	1.07	0.67	0.61	0.76	0.73	0.69	0.61	2.07	2.18	5.04	5.28	1.92	2.38	2.12	1.67	4.43	0.87	1.11	3.48	0.44	3.15	4.05
P ₂ O ₅	0.03	0.04	0.23	0.02	0.03	0.02	0.03	0.02	0.05	0.07	0.08	0.09	0.03	0.05	0.04	0.04	0.12	0.02	0.02	0.08	0.03	0.07	0.10	
LOI	0.90	0.60	0.60	1.80	1.20	1.20	1.10	1.50	1.00	2.40	2.80	4.10	4.20	1.60	2.00	1.80	1.50	2.30	0.60	1.20	2.60	0.90	1.30	2.60
SUM	99.55	99.15	99.46	99.43	99.55	99.49	99.23	99.65	99.48	99.63	99.56	99.67	99.63	99.44	99.80	99.79	99.64	99.70	99.77	99.78	99.65	99.81	99.77	99.74
Sc	2.0	3.0	2.0	2.0	2.0	2.0	2.0	2.0	2.0	10.0	10.0	20.0	21.0	3.0	10.0	8.0	5.0	13.0	1.0	2.0	16.0	4.0	13.0	16.0
V	12	12	10	11	14	b.d.	9	11	13	61	57	113	130	17	69	72	35	82	10	14	94	36	83	90
Cr	b.d.	b.d.	b.d.	b.d.	b.d.	b.d.	b.d.	b.d.	b.d.	68	62	103	123	b.d.	62	55	34	75	b.d.	b.d.	103	34	103	103
Ni	1.6	1.7	2.4	1.8	1.3	1.3	5.2	1.6	1.2	28.9	23.0	37.1	48.2	2.9	29.8	41.9	18.4	18.2	3.4	3.7	30.6	13.3	33.0	34.9
Cu	0.9	0.9	0.8	1.5	3.7	1.1	0.7	4.5	3.3	39	37	28	28	9.8	90	55	73	20	2.2	2.6	12	47	44	24
Rb	36.1	31.4	35.0	28.0	23.7	27.2	27.8	22.1	23.6	103	1158	219	221	60.0	103	114	80.4	158	31.5	42.4	162	42.2	137	198
Sr	16.2	26.1	18.7	12.1	10.7	8.3	8.6	4.2	3.6	142	188	114	88.5	39.7	116	153	102	126	7.4	3.5	127	176	128	160
Y	7.9	11.6	32.1	4.9	12.4	12.0	7.9	11.4	4.3	24.4	20.7	23.4	22.9	11.3	13.9	14.5	13.0	26.8	11.1	13.7	29.0	21.7	20.0	25.5
Zr	39.6	48.2	51.2	50.3	64.9	45.8	37.0	51.2	51.2	194	211	206	200	98.3	274	266	216	315	46.9	93.9	239	123	201	225
Nb	1.1	1.6	2.7	1.6	3.4	1.4	1.2	1.8	2.6	9.0	12.1	18.9	18.1	2.9	10.0	9.0	6.3	13.2	2.8	3.9	13.1	4.4	11.1	15.3
Ba	201	202	205	139	155	184	388	138	110	465	495	1216	1092	414	551	447	342	1097	160	187	709	69	648	844
La	11.3	14.7	54.0	13.0	19.1	15.4	10.5	11.7	5.4	30.4	41.4	31.1	17.8	14.5	21.9	17.0	31.3	16.1	25.7	14.3	28.1	42.7	25.8	
Ce	26.9	31.8	95.9	26.0	41.0	32.4	24.1	32.4	13.4	66.4	47.9	81.4	82.8	32.6	47.3	57.0	70.9	68.0	28.1	47.8	46.2	68.8	80.6	82.7
Pr	2.55	3.66	11.54	2.78	4.36	3.95	2.44	3.14	1.13	7.54	7.28	9.68	7.17	4.08	3.81	5.60	4.55	8.31	3.82	6.56	3.96	7.22	9.23	6.79
Nd	10.2	14.9	46.7	10.8	15.9	15.4	9.1	12.0	4.4	27.7	26.7	36.1	27.3	15.1	15.3	21.7	16.8	31.0	15.0	24.6	14.0	28.7	35.2	25.9
Sm	1.70	2.70	8.90	1.90	2.70	2.80	1.70	2.40	0.70	5.00	4.80	6.70	5.10	2.80	2.70	3.90	3.10	6.00	2.90	4.70	2.90	5.70	5.80	4.70
Eu	0.37	0.51	1.89	0.36	0.56	0.61	0.36	0.46	0.15	0.97	0.90	1.33	1.01	0.59	0.55	0.78	0.62	1.29	0.58	1.01	0.57	1.01	1.16	0.93
Gd	1.58	2.33	8.66	1.31	2.20	2.49	1.43	1.89	0.65	3.79	3.68	5.21	3.72	2.40	2.17	2.96	2.34	5.03	2.44	3.69	2.19	4.71	4.89	3.67
Tb	0.25	0.38	1.37	0.22	0.37	0.42	0.25	0.33	0.12	0.66	0.62	0.87	0.68	0.39	0.34	0.44	0.39	0.85	0.37	0.59	0.52	0.75	0.75	0.69
Dy	1.41	2.20	7.23	1.05	2.03	2.30	1.43	2.04	0.74	4.07	3.92	4.75	4.10	2.14	2.22	2.43	2.48	5.00	2.03	3.25	4.14	4.14	3.84	4.17
Ho	0.27	0.40	1.28	0.19	0.42	0.44	0.28	0.41	0.15	0.83	0.77	0.86	0.88	0.43	0.51	0.47	0.49	0.99	0.40	0.59	1.02	0.80	0.75	0.92
Er	0.80	1.16	3.45	0.59	1.27	1.30	0.79	1.23	0.51	2.46	2.49	2.75	2.59	1.23	1.67	1.48	1.54	3.00	1.16	1.63	3.36	2.30	2.02	2.81
Tm	0.12	0.18	0.50	0.09	0.19	0.19	0.12	0.18	0.08	0.35	0.38	0.43	0.40	0.17	0.28	0.24	0.26	0.45	0.16	0.23	0.51	0.33	0.32	0.42
Yb	0.84	1.15	3.15	0.55	1.23	1.16	0.80	1.24	0.56	2.33	2.48	2.89	2.60	1.19	1.94	1.59	1.69	3.19	1.08	1.49	3.46	2.21	2.10	2.80
Lu	0.13	0.17	0.41	0.08	0.18	0.16	0.12	0.18	0.09	0.35	0.38	0.46	0.41	0.18	0.30	0.26	0.26	0.50	0.17	0.20	0.51	0.32	0.32	0.43
Hf	1.3	1.3	1.6	1.3	1.7	1.4	0.9	1.7	1.3	5.2	6.2	6.2	6.0	3.0	7.1	7.8	6.3	8.7	1.4	2.6	6.5	3.7	5.8	6.7
Pb	5.3	7.6	17.4	4.3	5.0	3.2	5.7	1.9	4.0	44	7.4	4.3	3.7	3.6	4.0	4.2	4.5	5.7	3.9	5.3	4.8	3.6	3.8	6.2
Th	3.4	4.4	3.9	3.9	4.9	3.6	3.1	3.9	3.1	12.8	17.7	23.5	22.9	5.7	14.4	12.0	9.4	17.2	4.3	6.3	18.7	8.1	16.5	20.0
U	0.6	1.2	1.2	0.6	0.7	0.8	0.5	2.8	3.6	3.1	2.2	1.1	1.5	1.7	1.6	3.3	0.8	1.2	2.2	1.6	3.8	3.6	3.6	

	SiO ₂	53.63	54.14	54.41	50.50	95.30	94.18	89.29	56.16	95.11	97.65	95.21	79.75	65.68	61.09	73.10	96.39	84.73	73.63	72.92	77.43	71.00	75.25
TiO ₂	0.63	0.39	0.58	0.56	0.83	0.03	0.09	0.36	1.08	0.02	0.06	0.13	0.41	0.61	0.11	0.07	0.26	0.18	0.31	0.62	0.31	0.04	
Al ₂ O ₃	7.54	12.05	9.67	31.60	0.53	0.60	2.36	28.82	0.42	0.45	2.28	11.80	19.55	19.68	15.25	1.67	8.11	14.32	14.94	12.17	14.89	14.19	
Fe ₂ O ₃	14.68	8.47	12.53	2.22	2.59	4.43	5.12	1.37	1.54	0.48	0.16	0.85	2.22	4.62	1.92	0.60	1.76	2.67	2.65	2.22	3.24	1.57	
MnO	0.17	0.13	0.17	b.d.	b.d.	0.01	b.d.	b.d.	b.d.	b.d.	b.d.	0.02	0.03	0.05	0.04	b.d.	b.d.	0.02	0.02	0.02	0.05	0.01	
MgO	9.58	9.25	9.27	0.74	0.02	0.11	0.61	0.44	0.02	0.12	0.09	0.52	1.34	1.95	0.76	0.08	0.17	0.85	1.07	1.14	1.31	0.14	
CaO	9.85	9.32	7.98	0.17	0.01	0.02	0.02	0.10	b.d.	b.d.	b.d.	0.12	0.18	0.07	0.18	0.03	0.10	0.14	0.03	0.03	0.52	1.35	
Na ₂ O	1.84	2.12	3.34	0.79	0.04	0.04	0.04	0.73	0.02	b.d.	0.02	3.51	0.14	0.09	3.66	0.04	3.19	2.42	0.18	0.53	5.16	5.44	
K ₂ O	0.60	1.50	0.12	9.10	0.15	0.10	0.27	7.89	0.13	0.07	0.78	1.75	7.16	7.66	2.85	0.57	0.67	3.37	5.24	3.02	1.68	1.56	
P ₂ O ₅	0.12	0.07	0.08	0.07	0.01	0.03	0.10	0.10	0.02	0.02	0.03	0.15	0.07	0.04	0.02	0.04	0.02	0.01	0.02	0.12	b.d.		
LOI	1.10	2.20	1.60	4.10	0.30	0.30	1.80	3.90	1.30	1.00	1.20	1.40	2.90	3.90	1.90	0.40	0.80	2.20	2.40	2.70	1.60	0.30	
SUM	99.74	99.64	99.75	99.85	99.78	99.85	99.70	99.87	99.64	99.81	99.82	99.88	99.76	99.79	99.81	99.87	99.83	99.82	99.77	99.90	99.88	99.85	
Sc	23	28	21	34	6	1	3	16	11	1	2	2	5	12	1	1	1	2	6	11	3	b.d.	
V	136	189	145	222	6	10	43	102	13	11	10	16	63	52	12	5	24	9	44	40	18	b.d.	
Cr	1102	1232	814	198	27	136	89	164	34	48	34	21	21	55	b.d.	89	34	27	41	151	b.d.	b.d.	
Ni	55	60	70	0.7	4.0	23	76	1.9	4.5	13.8	2.3	9.4	3.3	15	6.3	1.7	2.5	4.7	2.0	24	13	5.2	
Cu	104.0	5.2	48.1	4.3	7.1	175	1055	7.8	1.4	58.6	3.9	1.6	5.6	0.9	1.9	8.7	4.5	3.2	12	2.8	2.7	6.8	
Rb	19.2	19.5	2.0	354	6.5	4.9	11.6	242	6.4	4.3	36.4	69	239	279	103	28.6	31.3	137	189	166	61.3	56.9	
Sr	39.3	81.2	63.0	51.7	2.2	32.6	12.5	35.7	1.7	0.8	6.6	82.6	22.9	15.1	105	6.7	61.0	77.6	17.5	38.6	157	240	
Y	17.9	20.7	17.7	39.0	13.2	4.7	22.7	14.1	16.9	7.7	6.8	5.5	8.3	19.2	2.9	8.9	6.1	5.0	5.9	17.7	5.6	1.0	
Zr	96	82	68	222	258	44.9	77.0	147	298	45.8	48.2	84.9	203	218	112	67.5	207	119	233	202	139	15.7	
Nb	4.0	6.0	3.0	12.8	16.5	0.8	2.0	9.7	24.1	1.5	2.0	3.7	12.1	16.4	3.9	1.9	3.7	5.4	7.1	10.7	9.5	2.3	
Ba	49	635	27	472	28	39	41	301	17	11	78	173	588	735	280	101	76	375	485	362	170	240	
La	5.1	15.6	15.6	2.0	2.0	4.1	16.4	16.1	0.9	2.1	4.9	18.3	21.7	33.9	51.7	8.8	21.8	50.6	12.5	48.0	14.5	2.3	
Ce	11.6	31.6	30.2	4.0	4.0	8.6	36.2	33.6	2.1	3.4	9.7	37.8	53.4	84.1	119.3	17.1	37.9	95.7	22.0	61.0	29.6	3.9	
Pr	1.50	3.33	3.14	0.53	0.45	1.04	4.11	4.42	0.22	0.44	1.15	3.70	4.52	9.18	8.97	2.07	4.07	9.07	2.89	11.01	3.13	0.40	
Nd	6.3	11.6	12.3	2.1	1.5	3.7	16.0	19.5	0.8	1.9	4.6	12.8	17.0	33.0	27.9	7.4	13.3	30.8	9.6	37.2	10.4	1.4	
Sm	2.1	2.5	2.6	0.9	0.3	0.8	3.3	4.4	0.3	0.3	0.9	1.8	2.5	5.8	3.0	1.5	1.9	4.0	1.7	6.0	1.9	0.2	
Eu	0.78	0.61	1.14	0.36	0.14	0.14	0.34	0.90	0.13	0.07	0.19	0.46	0.48	1.27	0.50	0.29	0.48	1.14	0.33	1.16	0.53	0.47	
Gd	2.49	2.55	2.85	1.97	0.70	0.55	3.40	3.03	0.73	0.69	0.97	1.16	1.99	3.68	1.06	1.38	1.32	1.85	1.16	4.13	1.48	0.22	
Tb	0.55	0.47	0.48	0.57	0.23	0.15	0.70	0.43	0.25	0.16	0.17	0.18	0.31	0.67	0.15	0.25	0.16	0.24	0.20	0.67	0.23	0.03	
Dy	2.99	2.92	2.76	4.53	1.92	0.86	4.20	2.08	2.08	1.10	1.05	0.85	1.53	3.87	0.56	1.53	0.85	0.91	0.80	3.20	1.13	0.16	
Ho	0.62	0.70	0.61	1.13	0.49	0.18	0.89	0.45	0.60	0.26	0.22	0.19	0.28	0.78	0.09	0.31	0.15	0.14	0.18	0.59	0.21	b.d.	
Er	1.64	1.87	1.68	3.66	1.52	0.49	2.63	1.38	2.06	0.78	0.64	0.55	0.74	2.58	0.31	0.88	0.56	0.37	0.43	1.72	0.65	0.07	
Tm	0.25	0.32	0.24	0.63	0.31	0.09	0.39	0.23	0.35	0.12	0.11	0.09	0.12	0.42	0.05	0.14	0.11	0.06	0.08	0.34	0.09	b.d.	
Yb	1.55	1.72	1.63	3.81	2.30	0.58	2.37	1.65	2.59	0.75	0.66	0.54	0.74	3.04	0.33	0.81	0.63	0.41	0.63	2.07	0.55	0.10	
Lu	0.19	0.26	0.20	0.58	0.32	0.08	0.33	0.28	0.42	0.11	0.10	0.09	0.11	0.44	0.06	0.12	0.10	0.07	0.12	0.32	0.08	0.02	
Hf	2.4	2.3	1.7	6.6	7.2	1.2	2.2	4.4	8.3	1.4	1.3	2.3	4.9	6.8	3.1	1.9	5.2	3.1	5.7	5.4	3.4	0.5	
Pb	1.0	7.0	0.6	1.5	1.3	1.1	0.6	2.4	1.0	0.4	0.5	1.4	1.6	2.2	2.1	1.3	1.3	1.5	1.1	2.5	1.3	6.1	
Th	5.6	5.9	1.6	17.2	6.3	1.1	3.6	72	5.9	1.4	2.2	5.6	8.3	23.3	13.8	5.7	6.8	8.6	14.0	13.1	6.5	0.6	
U	0.6	1.2	0.2	3.5	3.6	0.8	11.0	3.7	3.7	1.9	1.1	0.7	3.1	4.4	0.9	1.9	1.1	1.2	1.7	4.8	0.9	0.3	

Qtzt.=Quartzite; Scht.=Schist Phyl.=Phyllite; Ht. Sch.=Heterolithic Schist Ht. Qt.=Heterolithic Intercalated sandstone and fine siltstone inter band.

b.d.=below detection; Qtzt.=Quartzite; Scht.=Schist; Phyl.=Phyllite; Ht. Sch.=Heterolithic Schist; Amph.=Amphibolite; T.G.=Tonalite Gneiss.

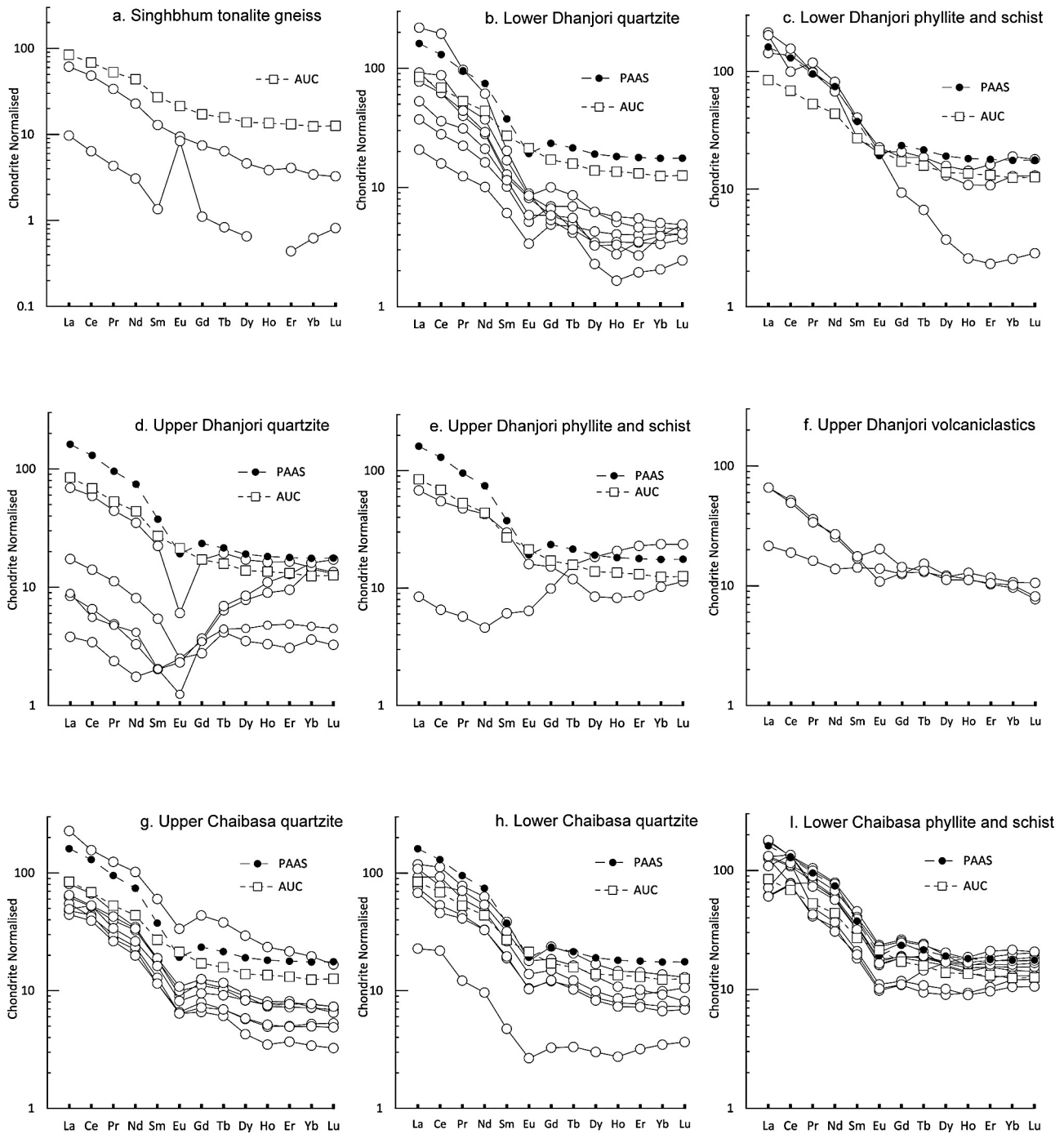


Fig. 8. Chondrite normalized REE plots of Dhanjori and Chaibasa clastics. See text for details.

mantle. In the case of the two samples this must have been before and after 2.5 Ga, e.g., some of the material in the Dhanjori samples was derived from the mantle later than 2.5 Ga, and consequently deposition of this mixed material must have occurred also later than 2.5 Ga.

As a reference isotopic framework for data interpretation we can assume a basement source with a Nd model age of 3.6 Ga (Table 3, tonalite sample S34), which is broadly consistent with the age of the basement in this part of the Singhbhum craton (Acharyya et al., 2010a; Hofmann and Mazumder, 2014). At 2.5 Ga, the assumed onset of deposition of Dhanjori sediments, the basement source had evolved to ε_{Nd} of -11, and at 2.2 Ga, the assumed deposition of Chaibasa to -15 (Table 3). Mantle-derived material at 2.5 Ga would

have had ε_{Nd} of +2.5 and at 2.2 Ga of +3 according to the DePaolo model (Fig. 12).

Using these isotopic estimates on the two major end member sources of sediment in the Dhanjori and Chaibasa basins, the Sm-Nd isotopic data in Table 3 provide some important constraints on the source compositions and the geological conditions under which deposition took place.

The Nd model ages of pelitic samples from the Dhanjori and Chaibasa Formations interpreted here in the sense of Taylor and McLennan (1985) as reliable large-scale samples of the exposed crust are surprisingly similar and cluster tightly around an average value of 2.5 Ga. This finding implies a supply of material from an isotopically uniform sedimentary source with respect to the

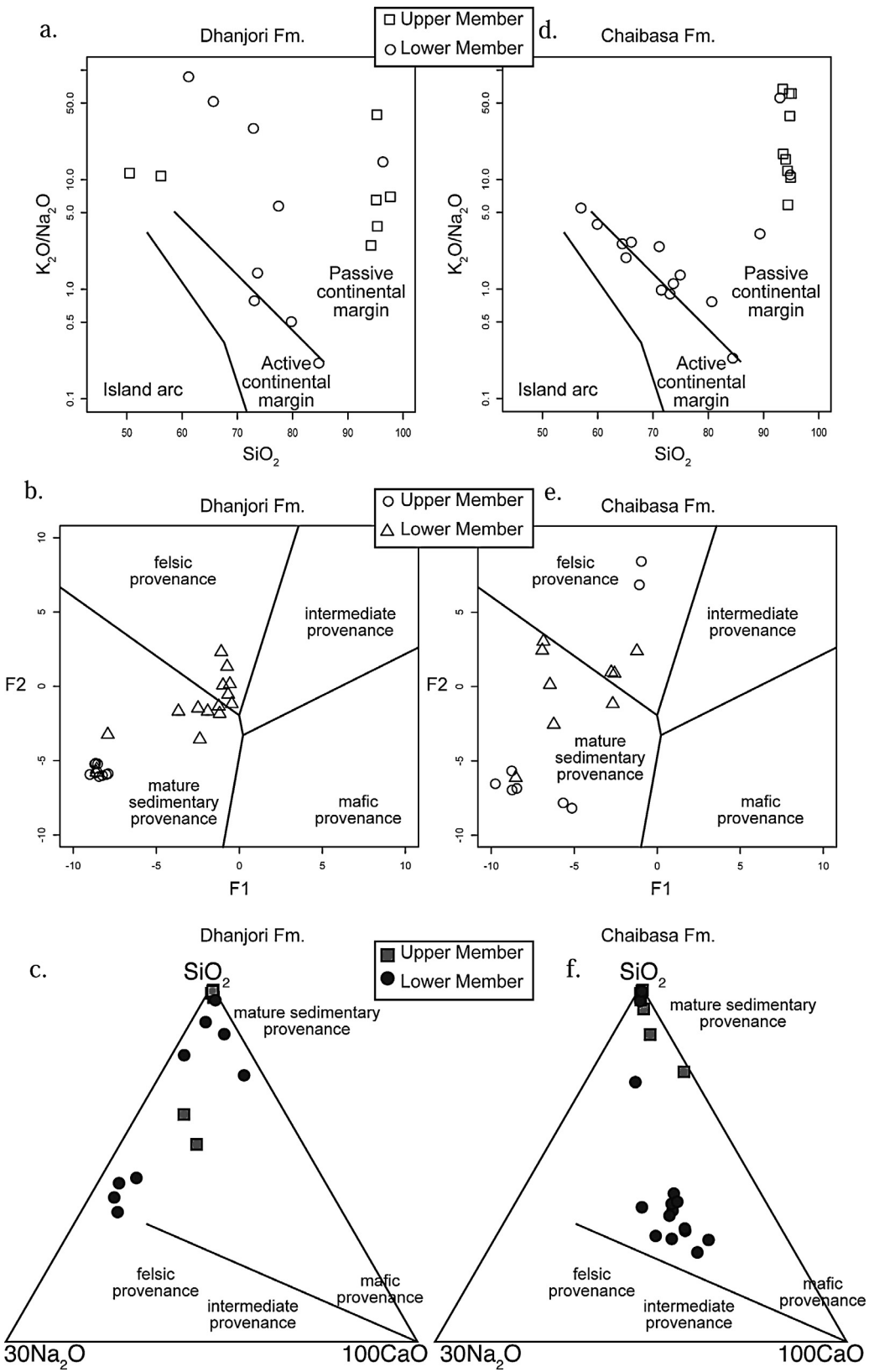


Fig. 9. Discriminant diagrams showing tectonic setting (after Roser and Korsch, 1986), and provenance (after Ohta, 2008). See text for details.

proportions of mantle-derived material and recycled older crust throughout the entire history of sedimentation. In detail it can be seen that the lower member of the Dhanjori Formation is isotopically more heterogeneous than the overlying Chaibasa Formation

in that it comprises older basement-derived material. The latter is preserved predominantly in the quartzites and a single phyllite sample (samples S1, S2, S8) that occur intercalated with juvenile mantle-derived first-order detritus (samples S4, R12). The quartzite

Table 3

Sm–Nd isotopic data for Palaeoproterozoic volcano-sedimentary Dhanjori and Chaibasa Formations of the Singhbhum mobile belt, east India.

Sample	Nd (ppm)	Sm (ppm)	$^{147}\text{Sm}/^{144}\text{Nd}$	$^{143}\text{Nd}/^{144}\text{Nd}$ (m)	$^{143}\text{Nd}/^{144}\text{Nd}$ (<i>t</i>)	$\varepsilon_{\text{Nd}}(t)$	t_{DM}
Chaibasa Fm. (<i>t</i> = 2.2 Ga)							
S 14 quartzite	13.36	2.529	0.1145	0.511413 ± 10	0.5096016	-0.7	2.51
S 17 quartzite	14.26	2.75	0.1164	0.511412 ± 6	0.509571	-1.3	2.56
S 21 Schist	18.52	3.42	0.1118	0.511358 ± 6	0.509590	-1.0	2.52
S 22 Schist	31.26	5.47	0.1058	0.511349 ± 7	0.509676	0.5	2.39
S 25 phyllite	34.47	6.244	0.1095	0.511342 ± 10	0.5096097	-0.7	2.49
S 30 Schist	16.40	2.88	0.1062	0.511364 ± 7	0.509684	0.7	2.39
S 27 Heterolithic	34.50	6.60	0.1158	0.511373 ± 7	0.509541	-1.9	2.60
S 11 Schist	36.09	6.65	0.1114	0.511306 ± 8	0.509544	-1.9	2.59
Dhanjori Fm. (<i>t</i> = 2.5 Ga)							
R 25 amphibolite	23.65	4.669	0.1194	0.510893 ± 9	0.5090041	-9.3	n.a.
S 08 Schist	22.78	5.54	0.1470	0.511765 ± 6	0.509439	-1.1	2.82 ^a
S 02 quartzite	16.67	2.943	0.1068	0.510824 ± 10	0.5091344	-6.6	3.20
S 04 phyllite	35.62	6.39	0.1084	0.511291 ± 5	0.509576	2.1	2.54
S 01 quartzite	27.85	3.204	0.06954	0.510010 ± 10	0.5089099	-10.5	3.61 ^a
R 12 phyllite	35.90	6.456	0.1087	0.511332 ± 11	0.5096124	2.8	2.48
Basement							
S 34 Singhbhum tonalite gneiss	12.63	2.208	0.1057	0.510568 ± 9	0.5088958	-14.8 (2.2 Ga) -11.3 (2.5 Ga)	3.61

m. = measured; *t* = initial value. $^{143}\text{Nd}/^{144}\text{Nd}$ are normalized to $^{146}\text{Nd}/^{144}\text{Nd} = 0.7219$. During the course of the study the La Jolla Nd standard solution yielded $^{143}\text{Nd}/^{144}\text{Nd} = 0.511847 \pm 8$ (2SD, *N* = 10). USGS granite standard G-2 yielded 52.98 ppm Nd, 7.08 ppm Sm; $^{147}\text{Sm}/^{144}\text{Nd} = 0.08085$, $^{143}\text{Nd}/^{144}\text{Nd} = 0.512214 \pm 2$ (2σ mean). t_{DM} = depleted-mantle model age according to DePaolo (1988).

^a 2-stage model age using $^{147}\text{Sm}/^{144}\text{Nd} = 0.115$ for first stage isotope evolution. N.a. = not applicable; Nd model age concept applies to crust-derived material.

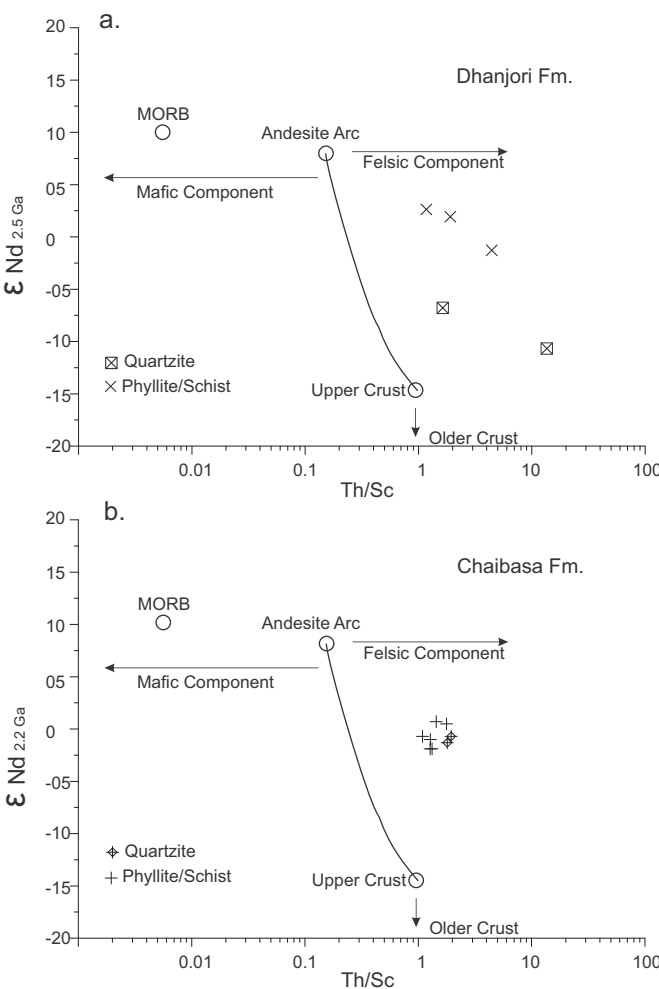


Fig. 10. ε_{Nd} –Th/Sc ratio plot of Dhanjori and Chaibasa clastic rock samples. See text for details.

data are interpreted as a signal from a spatially restricted source area as opposed to large-scale information in the phyllites. In the Chaibasa Formation, phyllite and also quartzite samples apparently were derived from a well-mixed and mostly juvenile provenance.

5. Discussions

The sedimentary facies characteristics of the Dhanjori Formation clearly indicate its generation in a continental (alluvial fan-fluvial) environment (Mazumder and Sarkar, 2004; Mazumder, 2005; Bhattacharya and Mahapatra, 2008; Mazumder et al., 2012b) and the associated mafic volcanics were formed in a continental rift setting (Mazumder and Arima, 2009; Fig. 13). The Chaibasa Formation is entirely marine with an overall shallowing up trend (Bose et al., 1997; Mazumder, 2005; Mazumder et al., 2012b, 2014; see section 4). There is no evidence of seismic deformation in the Dhanjori Formation. This indicates tectonic stability of the basin during Dhanjori sedimentation. The Dhanjori-Chaibasa transition indicates marine transgression in an intracontinental rift basin (Fig. 13) that subsequently turned into a tectonically active basin (Bose et al., 1997; Mazumder, 2005). The heterolithic and the shale facies of the lower Chaibasa member bear profuse penecontemporaneous deformation structures. Majority of these deformational structures have been interpreted as seismites (Bose et al., 1997; Bhattacharya and Bandyopadhyay, 1998; Mazumder, 2005; Mazumder et al., 2006, 2009, 2012b). Although commonly associated with compressional and orogenic zones, probably due to higher earthquake magnitude and damages produced in these tectonic settings, seismic deformation is common in marginal marine basins even in passive margin basins (Karig, 1971; Seth et al., 1990; Foix et al., 2008 and references therein). The mineralogical and textural maturity of the Chaibasa sandstone is also incompatible with its generation in a forearc setting (Busby and Ingersoll, 1995; Mazumder and Arima, 2013).

The uniform Nd model ages in the phyllites indicate a similar large-scale provenance and imply similar geological conditions for erosion and deposition of the Chaibasa and Dhanjori Formations. Regarding the question of the proportions of mantle-derived material and recycling of older crust in the basin, the finding that the

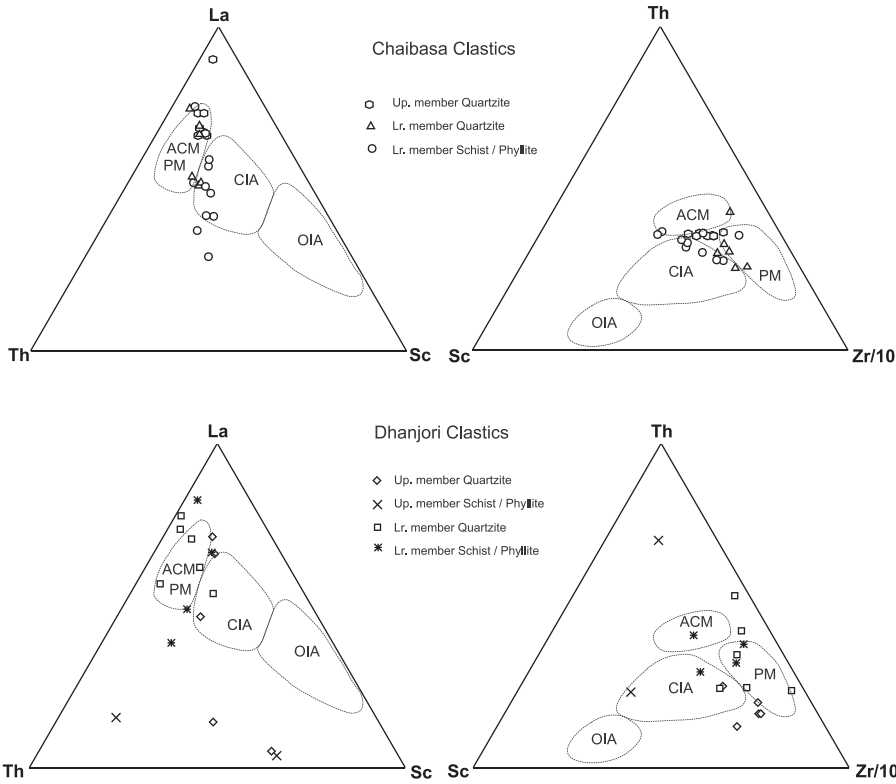


Fig. 11. La–Th–Sc and Th–Sc–Zr/10 plots of the meta-sedimentary rock samples from the Dhanjori and Chaibasa Formation (after [Bhatia and Crook, 1986](#)). OIA – oceanic island arc, CIA – continental island arc, ACM – active continental margin, and PM – passive continental margin.

Nd model ages are not much older than the inferred depositional ages of the material, indicates probably a provenance overwhelmingly dominated by mantle-derived material. Using the mixing parameter of [Patchett and Bridgwater \(1984\)](#) the phyllite samples comprise more than 90% juvenile material. Low $^{147}\text{Sm}/^{144}\text{Nd}$ ratios of 0.106–0.116 in the phyllites (except for sample S8, with a ratio of 0.147) reflects strongly enriched LREE patterns in the source rocks and confirms a granitic composition of the provenance. Areas of crust with high proportions of juvenile material can be found in island arcs and magmatic arcs on older crust. Considering that the sedimentary sequence of the Dhanjori Formation contains intercalated quartzite beds of which two samples yielded Nd model ages of 3.2 and 3.6 Ga, indicating mostly recycled basement material, the Nd isotopic data are best explained as evidence for a sedimentary

provenance in a juvenile felsic Andean-type magmatic arc situated on Archaean basement. This is also reflected in the $\varepsilon_{\text{Nd}}(t)$ vs. Th/Sc diagram ([Fig. 10](#)).

Interestingly, a subduction–accretion complex in the Singhbum during the Palaeo-Mesoarchaean time has been inferred by several authors ([Saha et al., 2004; Mukhopadhyay et al., 2012](#); see also [Prabhakar and Bhattacharya, 2013; Chaudhuri et al., 2015](#)). Based on their Sm–Nd isotope data, [Saha et al. \(2004\)](#) have inferred that the provenance of the late Archaean Birtola sandstone (see [Mazumder et al., 2012a](#) for discussion) formed in an island arc setting. The Sm–Nd model ages of the Birtola sandstones with respect to the depleted mantle (T_{DM}), range from 3.6 to 4.0 Ga, which was inferred as of an older sialic basement forming the root of the subduction complex at the base of 3.3 Ga amphibolites and

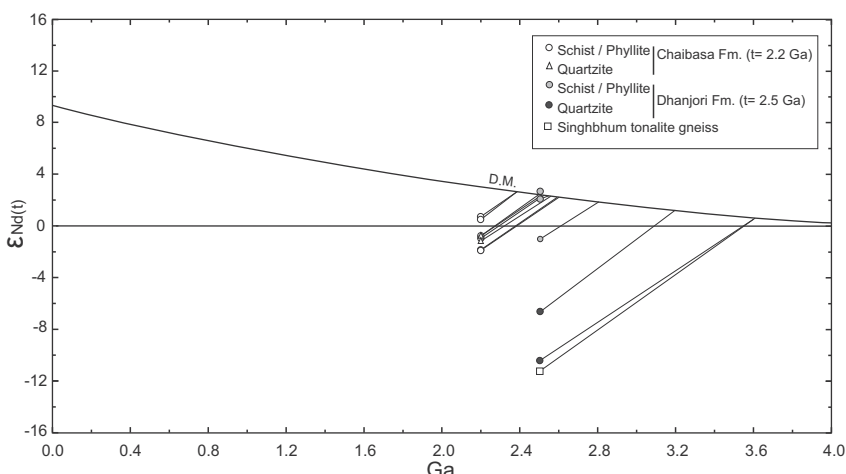


Fig. 12. ε_{Nd} -time plot of Singhbhum granitoid and selected Dhanjori and Chaibasa clastic rock samples. See text for details.

Table 4

Elemental ratios, weathering characteristics and maturity of Palaeoproterozoic Dhanjori and Chaibasa Formations, Singhbhum craton, eastern India.

Formation	S12	S13	S14	S15	S16	S17	S18	S19	S20	S21	S22	S23	S24	S25	S26	S27	S28	S29	S30	S31	S32	S33	S34	S35	S36		
Lithology	Upper member of Chaibasa Fm.																		Lower member of Chaibasa Fm.								
Lithology	Qtzt.	Qtzt.	Qtzt.	Qtzt.	Qtzt.	Qtzt.	Qtzt.	Qtzt.	Qtzt.	Qtzt.	Qtzt.	Qtzt.	Qtzt.	Qtzt.	Qtzt.	Qtzt.	Qtzt.	Qtzt.	Qtzt.	Qtzt.	Qtzt.	Qtzt.	Qtzt.	Qtzt.	Qtzt.	Qtzt.	
Zr/10	3.96	4.82	5.12	5.03	6.49	4.58	3.7	5.12	19.4	21.1	20.6	20	9.83	27.4	26.6	21.6	31.5	4.69	9.39	23.9	12.3	20.1	22.5				
Th/Sc	1.70	1.47	1.95	2.45	1.80	1.55	1.95	1.55	1.28	1.77	1.18	1.09	1.90	1.44	1.50	1.88	1.32	3.15	4.30	24.23	33.25	43.20	3.15	2.03	1.27	1.25	
Zr/Sc	19.80	16.07	25.60	25.15	32.45	22.90	18.50	25.60	25.60	19.40	21.10	10.30	9.52	32.77	27.40	46.90	46.95	14.94	30.75	15.46	14.06						
La/Sc	5.65	4.90	27.00	6.50	9.55	7.70	5.25	5.85	2.70	3.04	3.00	2.07	1.48	5.93	1.45	2.74	3.40	2.41	16.10	12.85	0.89	7.03	3.28	1.61			
CIA	63.70	58.32	57.79	77.72	76.40	70.52	64.75	78.42	74.96	63.20	61.52	69.74	71.70	57.51	63.73	61.32	58.84	63.82	69.09	71.16	70.62	52.05	68.44	67.35			
CIW	91.64	82.40	79.63	98.71	98.48	97.61	91.95	97.29	98.36	71.29	68.66	85.94	89.21	78.06	73.50	68.79	66.26	76.99	93.66	98.37	83.61	53.98	81.22	80.70			
ICV	0.769	0.917	0.918	0.566	0.636	0.694	0.879	0.526	0.659	0.880	0.799	0.757	0.829	0.846	0.915	0.837	0.793	0.778	0.806	0.804	1.079	0.836	0.817				
Formation	R6	R25	R22	R1	R21	R4	S01	S08	S09	S06	S07	S08	S05	S03	S06	S05	S02	S04	S01	R10	R11	R14	R13	R12	S34	R20	
Lithology	Upper member of Dhanjori Fm.																		Lower member of Dhanjori Fm.					Basement			
Lithology	Amph.	Amph.	Amph.	Amph.	Amph.	Amph.	Scht./Phyl.	Scht.	Qtzt.	Qtzt.	Qtzt.	Qtzt.	Qtzt.	Qtzt.	Qtzt.	Qtzt.	Qtzt.	Qtzt.	Qtzt.	Qtzt.	Qtzt.						
Zr/10	9.6	8.2	6.8	222	25.8	4.49	7.7	14.7	29.8	4.58	4.82	8.49	20.3	21.8	11.2	6.75	20.7	11.9	23.3	20.2	13.9	13.9	1.57				
Th/Sc	0.24	0.21	0.08	0.51	1.05	1.10	1.20	4.50	0.54	1.40	1.10	2.80	1.66	1.94	13.80	5.70	6.80	4.30	2.33	1.19	2.14	2.62					
Zr/Sc	4.17	2.93	3.24	6.53	43.00	44.90	25.67	9.19	27.09	45.80	24.10	42.45	40.60	18.17	112.00	67.50	207.00	59.50	38.83	18.36	46.33	39.25					
La/Sc	0.22	0.55	0.74	0.06	0.33	4.10	5.47	1.01	0.08	2.10	2.45	9.15	4.34	51.70	8.80	25.30	21.80	2.08	4.36	4.83	5.75	5.75					
CIA	25.89	35.33	32.45	73.39	68.27	74.04	85.68	74.39	68.65	80.30	71.80	59.94	70.18	69.67	61.78	69.37	64.50	71.27	74.37	56.96	52.01						
CIW	26.48	37.10	32.59	95.16	86.32	85.32	95.45	92.85	97.81	66.32	97.23	98.62	70.61	93.28	59.90	77.17	97.71	92.93	61.22	55.44							
ICV	4.931	2.577	3.497	0.430	6.868	7.883	2.606	0.378	6.667	1.578	0.491	0.583	0.586	0.762	0.622	0.832	0.758	0.672	0.635	0.621	0.820	0.711					

b.d. = below detection; Qtzt. = Quartzite; Scht. = Schist; Phyl. = Phyllite; Ht. Scht. = Heterolithic intercalated sandstone and fine siltstone inter band; Amph. = Amphibolite; T.G. = Tonalite Gneiss.
CIA = Chemical Index of Alteration, CIW = Chemical Index of Weathering ([Harms et al., 1988](#)), ICV = Index of Compositional Variability ([Cox et al., 1995](#)).

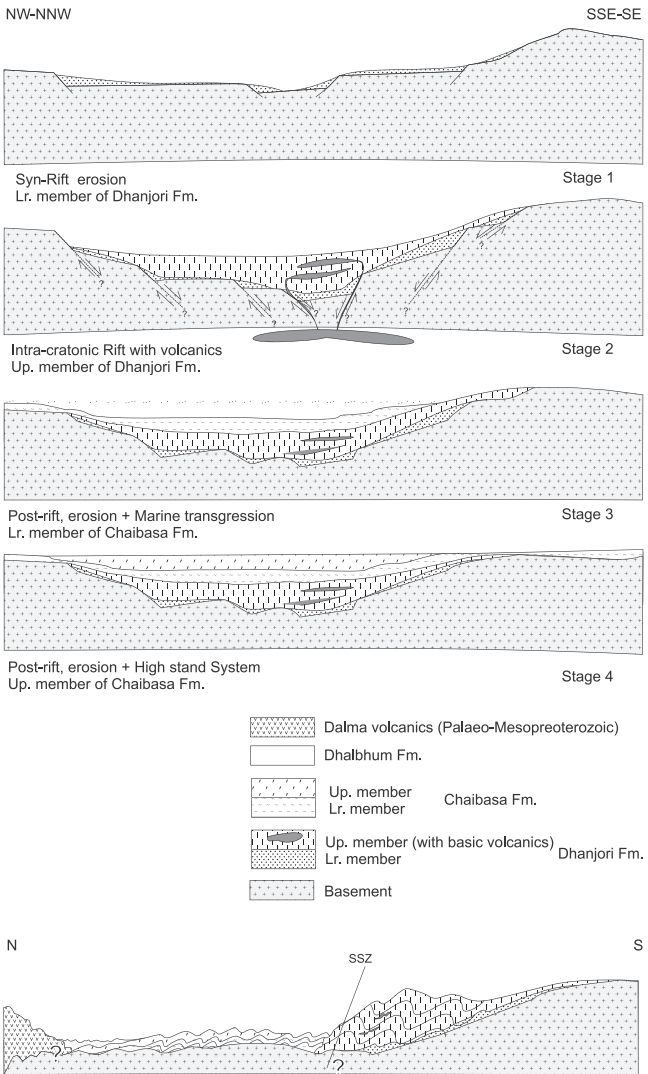


Fig. 13. Schematic diagram showing paleogeographic shift, tectonic evolution of the Dhanjori and Chaibasa Formations, Singhbhum craton, Eastern India and their present configuration. See text for details.

tonalities. [Mukhopadhyay et al. \(2012\)](#) have reported an interesting association of bedded chert, pillow lava, deep water dacitic lava, pyroclastics and BIF from the southern IOG (Fig. 2). Based on their sedimentological analysis in combination with major, trace and REE geochemistry, these authors have inferred an oceanic suprasubduction zone geodynamic setting during the southern IOG sedimentation ([Mukhopadhyay et al., 2012](#); see also [Chaudhuri et al., 2015](#)). Our Nd isotopic data thus corroborate the inference of a fore-arc basin setting on Singhbhum-type Mesoarchaean crust as proposed by earlier researchers.

Average ε_{Nd} ($t=2.2 \text{ Ga}$) = -0.8 ± 1.0 and average Nd model age (TDM) = $2.51 \pm 0.08 \text{ Ga}$ with average $^{147}\text{Sm}/^{144}\text{Nd}$ ratios = 0.1114 ± 0.0041 for phyllites and quartzites of the Chaibasa Formation (Table 2) indicate an extremely homogeneous source signature consistent with a late Archaean “juvenile” crustal provenance, possibly a dominantly upper crustal provenance. The Dhanjori samples are more heterogeneous, indicating probably proximal, poorly mixed provenance. The robust Nd isotopic data clearly indicate a mostly juvenile arc-related sedimentary provenance for both Dhanjori and Chaibasa sediments. On the other hand, sedimentary facies and stratigraphic analysis indicates a continental rift to marginal marine depositional setting for the Dhanjori and Chaibasa sediments (Fig. 13). The Sm-Nd

isotopic data, geochemical data in combination with previous sedimentological and stratigraphic analysis support a changing tectono-sedimentary regime from a Paleo/Mesoarchaean arc to Late Archaean-Palaeoproterozoic continental rift and subsequently, active marginal marine on the Singhbhum craton as suspected by Mazumder et al. (2012a,b).

6. Conclusions

Our new geochemical, petrographic and Sm–Nd isotopic data from the Late Archaean-Paleoproterozoic Singhbhum supracrustal succession (the Dhanjori and Chaibasa Formations) is entirely consistent with previous sedimentological data (Bose et al., 1997; Mazumder and Sarkar, 2004; Mazumder, 2005; Mazumder et al., 2012a,b) and confirms a terrestrial, rift-dominated tectonic setting for the Dhanjori Formation (proximal sources, poorly mixed provenance) and a marginal marine to offshore paleogeography in a tectonically active setting for more homogeneous Sm–Nd isotopic signature of the Chaibasa Formation (distal source, well mixed provenance).

Acknowledgements

This paper forms part of SD's doctoral dissertation under the supervision of RM and TB. SD gratefully acknowledges infrastructural facilities provided by the Geological Studies Unit, Indian Statistical Institute Kolkata and the Department of Geology, Calcutta University. SD and RM are grateful to the Department of Science and Technology, Government of India for financial support in form of a research fellowship and major research grant respectively. We are grateful to three anonymous reviewers, C. Fedo and R. Parrish for their critical but very helpful and constructive comments.

References

- Acharyya, S.K., 2003. A plate tectonic model for Proterozoic Crustal evolution of Central Indian Tectonic Zone. *Gondwana Geol. Mag.* 7, 9–31.
- Acharyya, S.K., Gupta, A., Orihashi, Y., 2010a. New U–Pb zircon ages from Palaeo-Mesoarchaean TTG gneisses of the Singhbhum Craton, eastern India. *Geochem. J.* 44, 81–88.
- Acharyya, S.K., Gupta, A., Orihashi, Y., 2010b. Neoarchaean–Palaeoproterozoic stratigraphy of the Dhanjori basin, Singhbhum Craton, Eastern India: and recording of a few U–Pb zircon dates from its basal part. *J. Asian Earth Sci.* 39, 527–536. <http://dx.doi.org/10.1016/j.jseas.2010.04.023>.
- Banerjee, S., Matin, A., 2013. Evolution of microstructures in Precambrian shear zones: an example from eastern India. *J. Struct. Geol.* 50, 199–208.
- Bhatia, M.R., Crook, K.A.W., 1986. Trace element characteristics of graywackes and tectonic setting discrimination of sedimentary basins. *Contrib. Miner. Pet.* 92, 181–193.
- Bhattacharya, H.N., 1991. A reappraisal of the depositional environment of the Precambrian metasediments around Ghatshila-Galudih, eastern Singhbhum. *J. Geol. Soc. India* 37, 47–54.
- Bhattacharya, H.N., Bandyopadhyay, S., 1998. Seismites in a Proterozoic tidal succession, Singhbhum, Bihar, India. *Sediment. Geol.* 119, 239–252.
- Bhattacharya, H.N., Mahapatra, S., 2008. Evolution of the Proterozoic rift margin sediments – North Singhbhum Mobile Belt, Jharkhand–Orissa, India. *Precambrian Res.* 162, 302–316.
- Bhattacharya, H.N., Nelson, D.R., Thern, E.R., Altermann, W., 2014. Petrogenesis and geochronology of the Arkasani Granophyre and felsic Dalma volcanic rocks: implications for the evolution of the Proterozoic North Singhbhum Mobile Belt, east India. *Geol. Mag.*, <http://dx.doi.org/10.1017/S0016756814000442>.
- Blair, T.C., McPherson, J.G., 1994. Alluvial fans and their natural distinction from rivers based on morphology, hydraulic processes, sedimentary processes, and facies assemblages. *J. Sediment. Res.* 64 (3), 450–489.
- Bose, M.K., 1994. Sedimentation pattern and tectonic evolution of the Proterozoic Singhbhum basin in the eastern Indian shield. *Tectonophysics* 231, 325–346.
- Bose, P.K., Mazumder, R., Sarkar, S., 1997. Tidal sandwaves and related storm deposits in the transgressive Proterozoic Chaibasa Formation, India. *Precambrian Res.* 84, 63–81.
- Bouvier, A., Vervoort, J.D., Patchett, P.J., 2008. The Lu–Hf and Sm–Nd isotopic composition of CHUR: constraints from unequilibrated chondrites and implications for the bulk composition of terrestrial planets. *Earth Planet. Sci. Lett.* 273, 48–57.
- Busby, C.J., Ingersoll, R.V., 579 pp. 1995. *Tectonics of Sedimentary Basins*. Blackwell Science, Oxford, UK.
- Chaudhuri, T., Mazumder, R., Arima, M., 2015. Petrography and geochemistry of Mesoarchaean komatiites from the eastern Iron Ore belt, Singhbhum Craton, India, and its similarity with 'Barberton type komatiite'. *J. Afr. Earth Sci.* 101, 135–147.
- Clark, C., Kinny, P.D., Harley, S.L., 2012. Sedimentary provenance and age of metamorphism of the Vestfold Hills, East Antarctica: evidence for a piece of Chinese Antarctica? *Precambrian Res.* 196, 23–45.
- Cox, R., Lowe, D.R., Cullers, R.L., 1995. The influence of sediment recycling and basement composition on evolution of mudrock chemistry in the southwestern United States. *Geochim. Cosmochim. Acta* 59, 2919–2940.
- Dasgupta, S., 2004. Modelling ancient orogens – an example from North Singhbhum Mobile Belt. Proceedings of the Workshop on (IGCP-453): Uniformitarianism Revised Edition on Orogenes of India. Geological Survey of India, Special Publications 84, 33–42.
- DePaolo, D.J., 1981. Neodymium isotopes in the Colorado Front Range and implications for crust formation in the Proterozoic. *Nature* 291, 193–197.
- DePaolo, D.J., 1988a. Age dependence of the composition of continental crust: evidence from Nd isotopic variations in granitic rocks. *Earth Planet. Sci. Lett.* 90, 263–271.
- DePaolo, D.J., 187 pp. 1988b. *Neodymium Isotope Geochemistry: An Introduction*. Springer-Verlag, New York.
- Elderfield, H., Greaves, M.J., 1982. The rare earth elements in seawater. *Nature* 296, 214–219.
- Eriksson, P.G., Condé, K.C., Trisgaard, H., Muller, W., Altermann, W., Catuneanu, O., Chiarenzali, J., 1998. Precambrian clastic sedimentation systems. *Sediment. Geol.* 120, 5–53.
- Eriksson, P.G., Mazumder, R., Catuneanu, O., Bumby, A.J., Ountsche Ilondo, B., 2006. Precambrian continental freeboard and geological evolution: a time perspective. *Earth-Sci. Rev.* 79, 165–204.
- Fedo, C.M., Eriksson, K.A., Krogstad, E.J., 1996. Geochemistry of shales from the Archean (~3.0 Ga) Buhwa Greenstone Belt, Zimbabwe: implications for provenance and source-area weathering. *Geochim. Cosmochim. Acta* 60, 1751–1763.
- Fedo, C.M., Young, G.M., Nesbitt, H.W., 1997. Paleoclimatic control on the composition of the Paleoproterozoic Serpent Formation, Huronian Supergroup, Canada: a greenhouse to icehouse transition. *Precambrian Res.* 86, 201–223.
- Foix, N., Paredes, J.M., Giacosa, R.E., 2008. Paleo-earthquakes in passive-margin settings, an example from the Paleocene of the Golfo San Jorge Basin, Argentina. *Sediment. Geol.* 205, 67–78.
- Ghosh, M., Mukhopadhyay, D., Sengupta, P., 2006. Pressure–temperature–deformation history for a part of the Mesoproterozoic fold belt in North Singhbhum, Eastern India. *J. Asian Earth Sci.* 26, 555–574.
- Gupta, A., Basu, A., 1991. Evolutionary trend of the mafic-ultramafic volcanism in the Proterozoic North Singhbhum mobile belt. *Indian Miner.* 45, 273–283.
- Gupta, A., Basu, A., 2000. North Singhbhum mobile belt, Eastern India – a review. *Spec. Publ. Geol. Survey India* 55, 195–226.
- Harnois, L., 1988. The CIW index: a news index of weathering. *Sediment. Geol.* 55, 319–322.
- Hegner, E., Klemd, R., Kröner, A., Corsini, M., Alexeiev, D.V., Iaccheri, L.M., Zack, T., Dulski, P., Xia, X., Windley, B.F., 2010. Mineral ages and P–T conditions of late Paleozoic high-pressure eclogite and provenance of mélange sediments in the South Tianshan Orogen of Kyrgyzstan. *Am. J. Sci.* 310, 916–950.
- Herron, M.M., 1988. Geochemical classification of terrigenous sands and shales from core or log data. *J. Sediment. Res.* 58, 820–829.
- Hofmann, A., Mazumder, R., 2014. A review of the current status of the Older Metamorphic Tonalite Gneiss: insight into the Palaeoarchean history of the Singhbhum craton, India. In: Mazumder, R., Eriksson, P.G. (Eds.), *Precambrian Basins of India: Stratigraphic and Tectonic Context*. Memoir Geological Society of London (in press), No. 43.
- Joy, S., Saha, D., 1998. Influence of micaceous impurity on dynamically recrystallized quartz c-axis fabric in L–S tectonites from the Singhbhum Shear Zone and its footwall, Eastern India. *J. Struct. Geol.* 20, 1509–1520.
- Joy, S., Saha, D., 2000. Dynamically recrystallised quartz c-axis fabrics in green-schist facies quartzites, Singhbhum shear zone and its footwall, eastern India – influence of high fluid activity. *J. Struct. Geol.* 22, 777–793.
- Karig, D.E., 1971. Origin and development of marginal basins in the Western Pacific. *J. Geophys. Res.* 76, 2542–2561.
- Mallik, L., Mazumder, R., Mazumder, B.S., Arima, M., Chatterjee, P., 2012. Tidal rhythmites in offshore shale: a case study from the Palaeoproterozoic Chaibasa shale, eastern India and implications. *Mar. Pet. Geol.* 30, 43–49.
- Mazumder, R., 1999. Imprint of wave reworking in early Proterozoic Chaibasa Sandstone. *J. Geol. Soc. India* 53, 615.
- Mazumder, R., 2000. Turbulence particle interactions and their implications for sediment transport and bedform mechanics under unidirectional current: some recent developments. *Earth Sci. Rev.* 50, 113–124.
- Mazumder, R., (PhD thesis; unpubl.) 2002. *Sedimentation History of the Dhanjori and Chaibasa Formations, Eastern India and its Implications*. Jadavpur University, Kolkata, India, 119 pp.
- Mazumder, R., 2004. Implications of lunar orbital periodicities from Chaibasa tidal rhythmite of late Paleoproterozoic age. *Geology* 32, 841–844.
- Mazumder, R., 2005. Proterozoic sedimentation and volcanism in the Singhbhum cratonic province, India and their implications. *Sediment. Geol.* 176, 167–193.
- Mazumder, R., Arima, M., 2005. Tidal rhythmites and their implications. *Earth Sci. Rev.* 69, 79–95.
- Mazumder, R., Arima, M., 2009. Implication of mafic magmatism in an intracontinental rift setting: a case study from the Palaeoproterozoic Dhanjori Formation, Singhbhum cratonic province, India. *J. Geol.* 117, 455–466.

- Mazumder, R., Arima, M., 2013. Tidal rhythm in deep sea environment: an example from Miocene Misaki Formation, Miura Peninsula. *Jpn. Mar. Pet. Geol.* 43, 320–325.
- Mazumder, R., Sarkar, S., 2004. Sedimentation history of the Palaeoproterozoic Dhanjori Formation, Singhbhum, India and its implications. *Precambrian Res.* 130, 267–287.
- Mazumder, R., Bose, P.K., Sarkar, S., 2000. A commentary on the tectono-sedimentary record of the pre-2.0 Ga continental growth of India vis-a-vis Pre-Gondwana Afro-Indian supercontinent. *J. Afr. Earth Sci.* 30, 201–217.
- Mazumder, R., van Loon, A.J., Arima, M., 2006. Soft sediment deformation structures in the Earth's oldest seismites. *Sediment. Geol.* 186, 19–26.
- Mazumder, R., Rodriguez-Lopez, J.A., Arima, M., van Loon, A.J., 2009. Palaeoproterozoic seismites (fine-grained facies of the Chaibasa Fm., E. India) and their soft-sediment deformation structures. In: Reddy, S.M., Mazumder, R., Evans, D.A., Collins, A.S. (Eds.), *Paleoproterozoic Supercontinent and its Global Evolution*. *Geol. Soc. Lond. Spec. Publ.* 323, 301–318.
- Mazumder, R., Eriksson, P.G., De, S., Bumby, A.J., Lenhardt, N., 2012a. Palaeoproterozoic sedimentation on the Singhbhum craton: global context and comparison with Kaapvaal. In: Mazumder, R., Saha, D. (Eds.), *Palaeoproterozoic of India*. *Geol. Soc. Lond. Spec. Publ.* 365, 51–76, <http://dx.doi.org/10.1144/SP365.4>.
- Mazumder, R., Van Loon, A.J., Mallik, L., Reddy, S.M., Arima, M., Altermann, W., Eriksson, P.G., De, S., 2012b. Mesoarchean-Palaeoproterozoic Stratigraphic Record of the Singhbhum Crustal Province, Eastern India: a synthesis. In: Mazumder, R., Saha, D. (Eds.), *Palaeoproterozoic of India*. *Geol. Soc. Lond. Spec. Publ.* 365, 31–49, <http://dx.doi.org/10.1144/SP365.3>.
- Mazumder, R., De, S., Ohta, T., Flannery, D., Mallik, L., Chaudhuri, T., Chatterjee, P., Ranaiyoson, M.A., Arima, M., 2014. *Palaeo-Mesoproterozoic sedimentation and tectonics of the Singhbhum Craton, eastern India, and implications for global and craton specific geological events*. In: Mazumder, R., Eriksson, P.G. (Eds.), *Precambrian basins of India: stratigraphic and tectonic context*. *Memoir Geological Society of London*, No. 43, In press.
- McLennan, S.M., Taylor, S.R., Eriksson, K.A., 1983a. Geochemistry of Archean shales from the Pilbara Supergroup, Western Australia. *Geochim. Cosmochim. Acta* 47, 1211–1222.
- McLennan, S.M., Taylor, S.R., Krone, A., 1983b. Geochemical evolution of Archean shales from South Africa. 1. The Swaziland and Pongola Supergroups. *Precambrian Res.* 22, 93–124.
- McLennan, S.M., Taylor, S.R., McGregor, V.R., 1984. Geochemistry of Archean metasedimentary rocks from West Greenland. *Geochim. Cosmochim. Acta* 48, 1–13.
- McLennan, S.M., Hemming, S., McDaniel, D.K., Hanson, G.N., 1993. Geochemical approaches to sedimentation, provenance and tectonics. In: Johnsson, M.J., Basu, A. (Eds.), *Processes Controlling the Composition of Clastic Sediments*, vol. 284. *Geological Society of America Special Paper*, Boulder, Colorado, pp. 21–40.
- McLennan, S.M., Taylor, S.R., Hemming, S., 2006. Composition, differentiation and evolution of continental crust: Constraints from sedimentary rocks and heat flow. In: Brown, M., Rushmer, T. (Eds.), *Evolution and Differentiation of the Continental Crust*. Cambridge University Press, pp. 92–134.
- Miall, A.D., 1996. *The Geology of Fluvial Deposits: Sedimentary Facies, Basin Analysis and Petroleum Geology*. Springer-Verlag Inc., Berlin, 582 pp.
- Mukhopadhyay, D., 1976. Present status of Precambrian Stratigraphy of Singhbhum – the problems and prospects. *Indian J. Earth Sci.* 3, 208–219.
- Mukhopadhyay, D., 1984. The Singhbhum Shear Zone and its place in the evolution of the Precambrian mobile belt of north Singhbhum. *J. Indian Soc. Earth Sci. CEISM*, 205–212.
- Mukhopadhyay, D., 2001. The Archaean nucleus of Singhbhum: the present state of knowledge. *Gondwana Res.* 4, 307–318.
- Mukhopadhyay, J., Ghosh, G., Zimmermann, U., Guha, S., Mukherjee, T., 2012. A 3.51 Ga bimodal volcanics-BIF-ultramafic succession from Singhbhum Craton: implications for Palaeoarchean geodynamic processes from the oldest greenstone succession of the Indian subcontinent. *Geol. J.* 47 (2–3), 284–311, <http://dx.doi.org/10.1002/gj.1314>.
- Mukhopadhyay, J., Crowley, Q.G., Ghosh, S., Ghosh, G., Chakrabarti, K., Misra, B., Heron, K., Bose, S., 2014. Oxygenation of the Archean atmosphere: new paleosol constraints from eastern India. *Geology*, <http://dx.doi.org/10.1130/G36091.1>.
- Naha, K., 1965. Metamorphism in relation to stratigraphy, structure and movements in parts of east Singhbhum, Eastern India. *Q. J. Geol. Miner. Metall. Soc. India* 37, 41–88.
- Nelson, D.R., Bhattacharya, H.N., Misra, S., Dasgupta, N., Altermann, W., 2007. New SHRIMP U-Pb zircon dates from the Singhbhum craton, Jharkhand–Orissa region, India. In: Banerjee, S. (Ed.), *International Conference on Precambrian Sedimentation & Tectonics & the Second GPSS Meeting*, Indian Institute of Technology, Bombay (Abstract).
- Nelson, D.R., Bhattacharya, H.N., Thern, E.R., Altermann, W., 2014. Geochemical and ion-microprobe U-Pb zircon constraints on the Archean evolution of Singhbhum Craton, eastern India. *Precambrian Res.* 255, 412–432.
- Nesbitt, H.W., Young, G.M., 2004. Ancient climatic and tectonic settings inferred from paleosols developed on igneous rocks. In: Eriksson, P.G., Altermann, W., Nelson, D.R., Mueller, W., Cataneau, O. (Eds.), *The Precambrian Earth: Tempos and Events. Developments in Precambrian Geology* 12. Elsevier, Amsterdam, pp. 482–493.
- Ohta, T., 2008. Measuring and adjusting the weathering and hydraulic sorting effects for rigorous provenance analysis of sedimentary rocks: a case study from the Jurassic Ashikita Group, south-west Japan. *Sedimentology* 55, 1687–1701.
- Pal, D.C., Chaudhuri, T., Mcfarlane, C.H., Mukharjee, A., Sarangi, A.K., 2011. Mineral chemistry and *in situ* dating of allanite, and geochemistry of its host rocks in the Bagjata Uranium Mine, Singhbhum Shear Zone, India: implications for the chemical evolution of REE mineralization and mobilization. *Econ. Geol.* 106, 1155–1171.
- Patchett, P.J., Bridgwater, D., 1984. Origin of continental crust of 1.9–1.7 Ga age defined by Nd isotopes in the Ketilidian terrain of South Greenland. *Contrib. Miner. Pet.* 87, 311–318.
- Pettijohn, F.J., 1975. *Sedimentary rocks*, vol. 7., 3rd ed. Harper International, Tulsa, Oklahoma, 628 pp.
- Potter, P.E., Maynard, J.B., Depetris, P.J., 2005. *Mud and Mudstones Introduction and Overview*. Springer-Verlag.
- Prabhakar, N., Bhattacharya, A., 2013. Palearchean partial convective overturn in the Singhbhum Craton, Eastern India. *Precambrian Res.* 231, 106–121.
- Reddy, S.M., Clarke, C., Mazumder, R., 2009. Temporal constraints on the evolution of the Singhbhum Crustal Province from U-Pb SHRIMP data. In: Saha, D., Mazumder, R. (Eds.), *Paleoproterozoic Supercontinents and Global Evolution*. International Conference on Paleoproterozoic Supercontinents and Global Evolution Abstract Volume. International Association for Gondwana Research, Conference Series, vol. 9, pp. 17–18.
- Rollinson, H.R., 1993. *Using Geochemical Data: Evaluation, Presentation, Interpretation*. Longman, Harlow.
- Rollinson, H.R., 2007. *Early Earth Systems: A Geochemical Approach*. Blackwell Publishing Ltd, 298 pp.
- Roser, B.P., Korsch, R.J., 1986. Determination of tectonic setting of sandstones mudstones suites using SiO₂ content and K₂O/Na₂O ratio. *J. Geol.* 94, 635–650.
- Roser, B.P., Korsch, R.J., 1988. Provenance signatures of sandstone–mudstone suites determined using discriminant function analysis of major-element data. *Chem. Geol.* 67, 119–139.
- Roy, A., Sarkar, A., Jeyakumar, S., Aggrawal, S.K., Ebihara, M., 2002. Sm–Nd age and mantle characteristics of the Dhanjori volcanic rocks, Eastern India. *Geochem. J.* 36, 503–518.
- Saha, A.K., 1994. Crustal evolution of Singhbhum–North, Orissa, eastern India. *Geol. Soc. India Mem.* 27, 341 pp.
- Saha, A., Basu, A.R., Garzzone, C., Bandyopadhyay, P.K., Chakrabarti, A., 2004. Geochemical and petrological evidence for subduction accretion processes in the Archean Eastern Indian Craton. *Earth Planet. Sci. Lett.* 220, 91–106.
- Sarkar, S.C., 1984. *Geology and Ore Mineralisation of the Singhbhum Copper–Uranium Belt*, Eastern India. Jadavpur University, Calcutta.
- Sarkar, S.C., Deb, M., 1971. Dhanjori basalts and some related rocks. *Q. J. Geol. Miner. Metall. Soc. India* 43, 29–37.
- Sarkar, S.N., Saha, A.K., 1962. A revision of the Precambrian stratigraphy and tectonics of Singhbhum and adjacent region. *Q. J. Geol. Miner. Metall. Soc. India* 34, 97–136.
- Sarkar, S.N., Ghosh, D.K., Lambert, R.J.St., 1986. Rubidium–Strontium and lead isotopic studies of the Soda granites from Musaboni area, Singhbhum Copper Belt. In: Sarkar, S.N., Associates (Eds.), *Geology and Geochemistry of Sulphide Ore bodies and Associated Rocks in Musaboni and Rakha Mines Section in the Singhbhum Copper Belt. Diamond Jubilee Monograph*, Indian School of Mines, Dhanbad, pp. 101–110.
- Sengupta, S., Chattopadhyay, B., 2004. Singhbhum Mobile Belt – how far it fits an ancient Orogen. *Geol. Survey India Spec. Publ.* 84, 24–31.
- Seth, A., Sarkar, S., Bose, P.K., 1990. Synsedimentary seismic activity in an immature passive margin basin (lower member of the Katrol Formation, Upper Jurassic, Kutch, India). *Sediment. Geol.* 68, 279–291.
- Sugitani, K., Yamashita, F., Nagaoka, T., Yamamoto, K., Minami, M., Mimura, K., Suzuki, K., 2006. Geochemistry and sedimentary petrology of Archean clastic sedimentary rocks at Mt. Goldsworthy, Pilbara Craton, Western Australia: evidence for the early evolution of continental crust and hydrothermal alteration. *Precambrian Res.* 147 (1–2), 124–147, <http://dx.doi.org/10.1016/j.precamres.2011.11.001>.
- Taylor, S.R., McLennan, S.M., 1985. *The Continental Crust: Its Composition and Evolution*. Blackwell, London, pp. 312.
- Taylor, S.R., McLennan, S.M., 1995. The geochemical evolution of the continental crust. *Rev. Geophys.* 33, 241–265.
- Van de Kamp, P.C., Leake, B.E., 1985. Petrography and geochemistry of feldspathic and mafic sediments of the northeastern Pacific margin. *Trans. R. Soc. Edinburgh: Earth Sci.* 76, 411–499.
- Wilde, P., Quinby-Hunt, M.S., Erdtmann, B.D., 1996. The whole-rock cerium anomaly: a potential indicator of eustatic sea-level changes in shales of the anoxic facies. *Sediment. Geol.* 101 (1), 43–53.